Ministry of Water Resources

Bangladesh Water Development Board

Coastal Embankment Improvement Project, Phase-I (CEIP-I)

Long Term Monitoring, Research and Analysis of Bangladesh Coastal Zone (Sustainable Polders Adapted to Coastal Dynamics)

Coastal erosion at Kuakata sea beach

Joint Venture of DHI The expert in WATER ENVIRONMENTS & Deltares Enabling Delta Life

in association with IWM, Bangladesh and University of Colorado, Boulder and Columbia University

Ministry of Water Resources

Bangladesh Water Development Board

Coastal Embankment Improvement Project, Phase-I (CEIP-I)

Long Term Monitoring, Research and Analysis of Bangladesh Coastal Zone (Sustainable Polders Adapted to Coastal Dynamics)

Coastal erosion at Kuakata sea beach

June 2022

Joint Venture of DHI & Deltares in association with IWM, Bangladesh and University of Colorado, Boulder and Columbia University

Bangladesh Water Development Board
Coastal Embankment Improvement Project, Phase-I (CEIP-I)

Long Term Monitoring, Research and Analysis of Bangladesh Coastal Zone

Office: Flat #3/B, House #4, Road #23/A, Banani, Dhaka 1213, BANGLADESH Phone +880 1307 693299

Memo No: CEIP/LTMRA/0622/185 30 June 2022

Project Management Unit
Coastal Embankment Improvement Project, Phase-I (CEIP-I)
Pani Bhaban, Level-10
72, Green Road, Dhaka-1205

Attn: Mr. Syed Hasan Imam, Project Director

Dear Mr Imam,

Subject: Submission of the report Titled "Coastal erosion at Kuakata sea beach".

It is our pleasure to submit herewith five copies of the report titled ***"Coastal erosion at Kuakata sea beach"***.

This report deals with modelling of coastal erosion for a pilot case. The on-going erosion at Kuakata sea beach has been chosen as pilot case. The focus of the present study has been to provide an understanding of the causes for the on-going erosion on the stretch of coast between the Andharmanik River and the Gangamati River.

Thanking you,

Yours sincerely,

Dr Ranjit Galappatti
Team Leader

Copies: Engineer Fazlur Rashid, Director General, BWDB
Dr. Zia Uddin Baig, ADG (Planning), BWDB
Dr Kim Wium Olesen, Project Manager, DHI
Ms. Sonja Pans, Deltares Project Manager
Mr Zahirul Haque Khan, Deputy Team Leader
Mr AKM Bodruddoza, Procurement Specialist
Swarna Kazi, Sr. Disaster Risk Management Specialist, World Bank

Contents

1 **Introduction** 1

2 **Available data** 3
2.1 Historical coastlines 3
2.2 Coastal profiles 3
2.3 ADCP measurements 4
2.4 Water level measurements 5
2.5 Borehole data 5

3 **Methodology** 7

4 **Site visit** 9
4.1 Section 1 9
4.2 Section 2 10
4.3 Section 3 11
4.4 Section 4 12
4.5 Section 5 12
4.6 Section 6 13

5 **Analysis of morphological evolution** 15
5.1 Shoreline evolution 15
5.2 Profile evolution 18

6 **Spectral wave modelling** 25
6.1 Model description 25
6.2 Results 29

7 **Littoral drift modelling** 33
7.1 Model description 33
7.2 Results 34

7.2.1 Direction of littoral drift 34

7.2.2 Temporal variation 35

7.2.3 Distribution of littoral drift in the coastal profile 37

8 **Discussion** 39
8.1 Summary of findings 39
8.2 Limitations of the present work and suggestions for further studies 39
8.3 Discussion of coastal protection strategies 40

9 **References** 43

A **Flow fields over the sandbars in the Pussur River** 1

FIGURES

Figure 1 Satellite image showing the location of available historical coastlines. Image credit: Modified Copernicus Sentinel data 2022/Sentinel Hub ... 3
Figure 2 Overview of the data collected during the 2020 topgraphic and bathymetric survey. Profiles are numbered 1 to 86 with number 1 being the most westerly. Image credit: Modified Copernicus Sentinel data 2022/Sentinel Hub ... 4
Figure 3 Overview of the data collected during the 2022 topgraphic and bathymetric survey. Image credit: Modified Copernicus Sentinel data 2022/Sentinel Hub ... 4
Figure 4 Satellite image showing the locations of the ADCPs deployed during the 2018 (orange) and the 2020 (green) campaigns. Image credit: Modified Copernicus Sentinel data 2022/Sentinel Hub ... 5
Figure 5 Satellite image showing the location of boreholes extracted in the 2020 geological survey. Illustration taken from ref. /1/. ... 6
Figure 6 Overview of the stretch of coast that was inspected during the site visit. Coloured lines indicate the extent of coastal sections. ... 9
Figure 7 Photos of the beach at the eastern end (top) and the western end (bottom) of coastal section 1. ... 10
Figure 8 Photos showing the beach and revetment along section 2. Note that the photos were taken close to low tide ... 11
Figure 9 Photo showing geotextile bags on the beach at section 3. ... 12
Figure 10 Photo showing the beach at section 4. ... 12
Figure 11 Photo showing the beach at section 5. ... 13
Figure 12 Photos of the beach at section 6. ... 14
Figure 13 Satellite image showing the positions of historical shorelines as well as the baseline (white) used to perform the historical shoreline analysis. Numbers indicate distance (in km) along the baseline. Image credit: Modified Copernicus Sentinel data 2022/Sentinel Hub ... 15
Figure 14 Historical coastline positions at 3 locations along the coast. Shoreline position indicates the orthogonal distance from the baseline to the water line (positive in the offshore direction). ... 16
Figure 15 10-year average rates of change in coastline position. Positive values indicate shoreline advance ... 17
Figure 16 Littoral drift estimated from observed shoreline changes. Positive values indicate drift towards the west. ... 18
Figure 17 Profile plots showing the bed levels along the full length of profile 1 (top) and profile 20 (bottom) located at km 1.5 and km 5 respectively. ... 18
Figure 18 Profile plots showing the inner part of four of the profiles measured during the 2020 survey ... 20
Figure 19 Comparison of 2020 and 2022 survey data from profile 14 (3.8 km). Top: Profile view showing elevation as a function of cross shore distance. Bottom: Plan view showing longshore location as function of cross shore distance. ... 21
Figure 20 Comparison of 2020 and 2022 survey data from profile 20 (5.0 km). Top: Profile view showing elevation as a function of cross shore distance. Bottom: Plan view showing longshore location as function of cross shore distance. ... 22
Figure 21 Comparison of 2020 and 2022 survey data from profile 26 (6.2 km). Top: Profile view showing elevation as a function of cross shore distance. Bottom: Plan view showing longshore location as function of cross shore distance. ... 22
Figure 22 Comparison of 2020 and 2022 survey data from profile 50 (11.6 km). Top: Profile view showing elevation as a function of cross shore distance. Bottom: Plan view showing longshore location as function of cross shore distance. ... 23
Figure 23 Bathymetry plot showing the extent of the model domain used for the spectral wave model. ... 25
Figure 24 Plot of the mesh used for the SW model showing the mesh resolution in the area around Kuakata. ... 26
Figure 25 Comparison of measured water levels at Ratnabad outfall (blue) and synthesized water levels at Kuakata (black). ... 26
Figure 26 Time series plots comparing modelled (red) and measured (black) wave parameters during the 2018 offshore ADCP deployment. ... 28
Figure 27 Time series plots comparing modelled (red) and measured (black) wave parameters for the 2020 offshore ADCP deployment. ... 28

Figure 28 Time series plots comparing modelled (red) and measured (black) wave parameters for the 2018 nearshore ADCP deployment. 29
Figure 29 Satellite image showing the locations of profiles (pink dots) where wave conditions were extracted and littoral drift calculations were performed. White numbers indicate distance along baseline in km. Image credit: Modified Copernicus Sentinel data 2022/Sentinel Hub 29
Figure 30 Wave roses showing the modelled wave conditions at points a (left), b (centre) and c (right). 30
Figure 31 Scatterplot showing modelled significant wave heights and peak wave periods at the location of profile 34. The red dot indicates the wave height ($H_{s,12}$) and period ($T_{p,12}$) exceeded 12 hours a year. 31
Figure 32 Effect of varying bed roughness on littoral drift calculated for profile 23 (one-year period in 2016). 34
Figure 33 Examples of Q-alpha curves showing how the net (blue lines) and gross (red lines) littoral drift varies with coastline orientation. Black dots indicate the present coastline orientations. 35
Figure 34 Overview of the temporal variation in littoral drift. For each profile the top panel shows the significant wave height and the bottom panel shows the littoral drift. Littoral drift is illustrated as a time-series of yearly accumulated net transport (black lines), yearly gross (red bars) and net (blue bars) littoral drift. 36
Figure 35 Profile plot showing the bed level and calculated net littoral drift in profile 23 (km 5.6). 37

TABLES

Table 1 List of settings for the MIKE 21 spectral wave model 27

Table 2 Summary of the results from the LITDRIFT modelling 34

APPENDICES

Appendix A Coastal profile plots

1 Introduction

The main objective of the “long-term monitoring, research and analysis of the Bangladesh coastal zone” project is to create a framework for polder design to support sustainable polder management, based on understanding of the long-term and large scale dynamics of the delta. The modelling work within the project is carried out to improve our understanding of the long-term and large-scale dynamics of the Ganges-Brahmaputra-Meghna (GBM) delta. There is insufficient knowledge about sediment budgets in the delta. This includes sediment input, transport and distribution in the river system and the estuaries. The knowledge on hydrodynamics and sediment dynamics, at present and in the future under climate change and human interventions is essential for the framework of polder design.

This report deals with modelling of coastal erosion for a pilot case. Coastal erosion is one of the key threats to polders in the lower GBM delta. The on-going erosion at Kuakata sea beach has been chosen as pilot case. Kuakata sea beach located on the southern side of Kolapara has been eroding rapidly over the past decades and the erosion is now threatening to damage important assets. A primary concern is the stability of the bank protection for polder 48 which runs along the shore west of Kuakata. In several locations, shoreline retreat has meant that the bank protection is now exposed to wave action and has stated to fail.

The focus of the present study has been to provide an understanding of the causes for the on-going erosion on the stretch of coast between the Andharmanik River and the Gangamati River. This is done through a two-sided approach. On one side, the actual erosion is assessed through an analysis of historical coastlines and coastal profiles providing quantification of the historical erosion and an estimate of the magnitude of the littoral drift. On the other side a suite of numerical models were set up to simulate wave conditions and littoral drift providing an understanding of the mechanisms that cause the observed erosion.

The present report is structured as follows. Section 2 provides an overview of all the data used in the present study and section 3 then presents methodology chosen based on what data was available. Section 4 provides a description of the considered coast based on observations made during a recent site visit. Section 5 presents the performed analysis of coastal profiles and coastlines. Sections 6 and 7 present the setup and results of numerical models simulating waves and littoral drift. Lastly, section 7 summarises the findings of the study, discusses the results and provides recommendations for their application and for further studies.

2 Available data

This section describes the overall properties of the available data in terms of temporal and spatial coverage, parameters etc. Analyses of the data are presented in the relevant parts of sections 4 – 7.

2.1 Historical coastlines

Based on Landsat imagery from USGS Earth Explorer, IWM has digitized historical coastlines of the coast around Kuakata. For this purpose, the coastline was defined as the water line and the recorded coastline positions are therefore affected by water level variations (e.g. tidal and seasonal). The digitized coastlines cover the period 1990 until 2022 with data for every 5 years in the 1990'ies and every year since 2000.

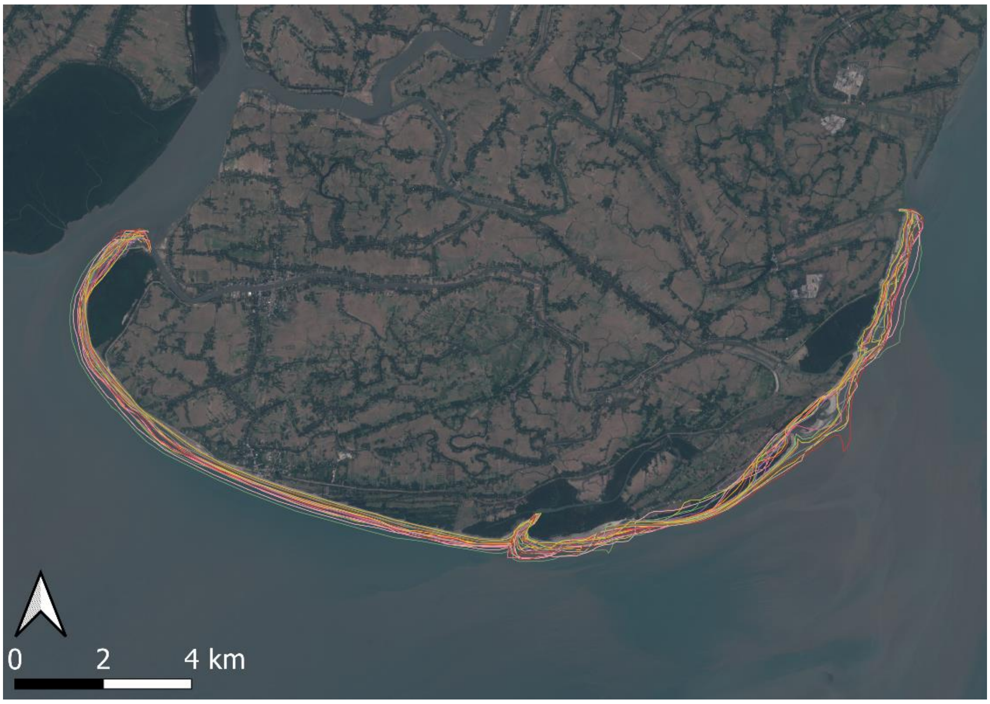

Figure 2-1 Satellite image showing the location of available historical coastlines. Image credit: Modified Copernicus Sentinel data 2022/Sentinel Hub

2.2 Coastal profiles

Topographic and bathymetric data from the coast around Kuakata is available from two surveys carried out in 2020 and 2022:

- Between January and March 2020, IWM carried out an extensive bathymetric and topographic survey of the south coast of Kolapara and the area further south. The survey was done along 86 lines covering the beach and extending up to 30 km offshore (Figure 2-1).
- Another smaller survey was carried out in March 2022 in order to determine possible changes in the nearshore parts of some of the profiles measured in 2020. Thus 12 profiles were measured each of which extended out to approximately 300 m offshore (Figure 2-3).

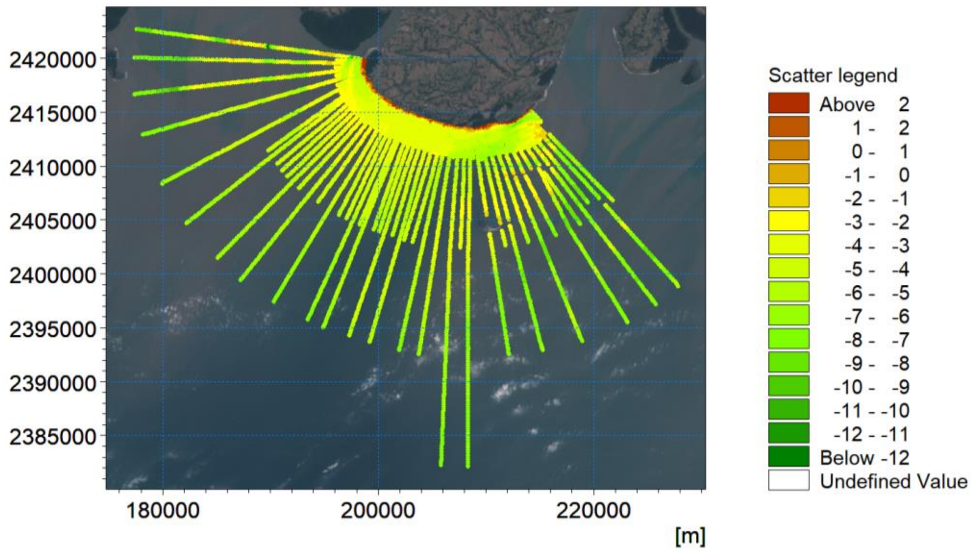

Figure 2-2 Overview of the data collected during the 2020 topgraphic and bathymetric survey. Profiles are numbered 1 to 86 with number 1 being the most westerly. Image credit: Modified Copernicus Sentinel data 2022/Sentinel Hub

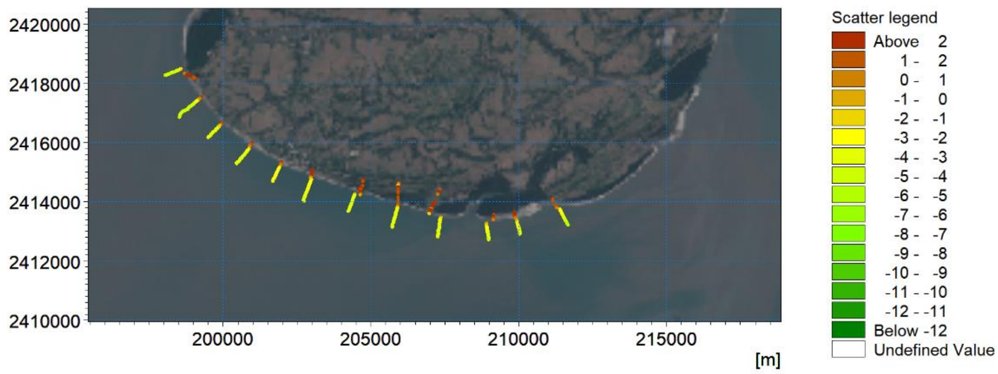

Figure 2-3 Overview of the data collected during the 2022 topgraphic and bathymetric survey. Image credit: Modified Copernicus Sentinel data 2022/Sentinel Hub

2.3 ADCP measurements

Data is available from two measurement campaigns each of which measured waves, currents and water levels at two locations using bottom mounted acoustic doppler current profilers (ADCP). The first campaign was carried out in March and April 2018 (1 month duration) and had one ADCP deployed in the Rabnabad Channel east of Kolapara and one ADCP deployed approximately 20 offshore (Figure 2-4). The second campaign was carried out in February and March 2020 (10 days duration) and had one ADCP located in the Rabnabad Channel and one deployed approximately 50 km offshore.

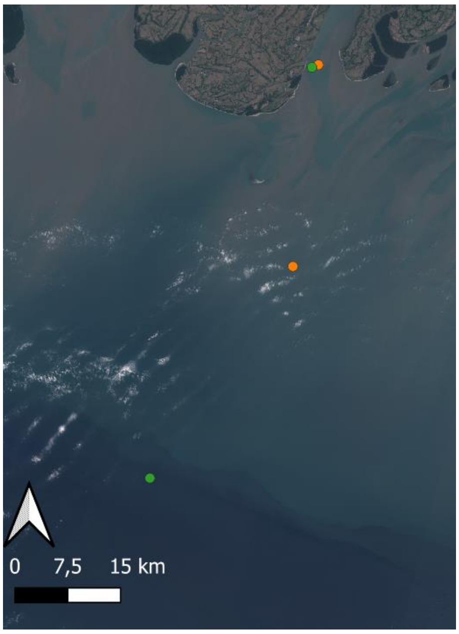

Figure 2-4 Satellite image showing the locations of the ADCPs deployed during the 2018 (orange) and the 2020 (green) campaigns. Image credit: Modified Copernicus Sentinel data 2022/Sentinel Hub

2.4 Water level measurements

A large number of water level gauges are distributed across Bangladesh. The one closest to Kuakata is located on the eastern side of Kolapara. A 1-year time series from 2019 and 2020 is available from this location.

2.5 Borehole data

In June 2020, an extensive geological survey was carried out during which boreholes were extracted from 16 locations along the Kuakata coastline (Ref /1/, appendix 6). As shown in Figure 2-5, 13 of these boreholes were extracted on the dry beach and 3 were extracted from the seabed close to shore.

Sediment grain size analysis of the borehole cores generally showed that the upper soil layers (down to a level of between -6m and -12 m) consisted of well sorted fine sand with a median grain size typically around 0.1 mm. Some boreholes (9, 10, 11, 13 and 15), however, showed a thinner layer (less than 2 m thick) of soft to stiff clay on top of the sand layer. These finer deposits appear to be quite scattered, and the coast is therefore considered to be essentially sandy.

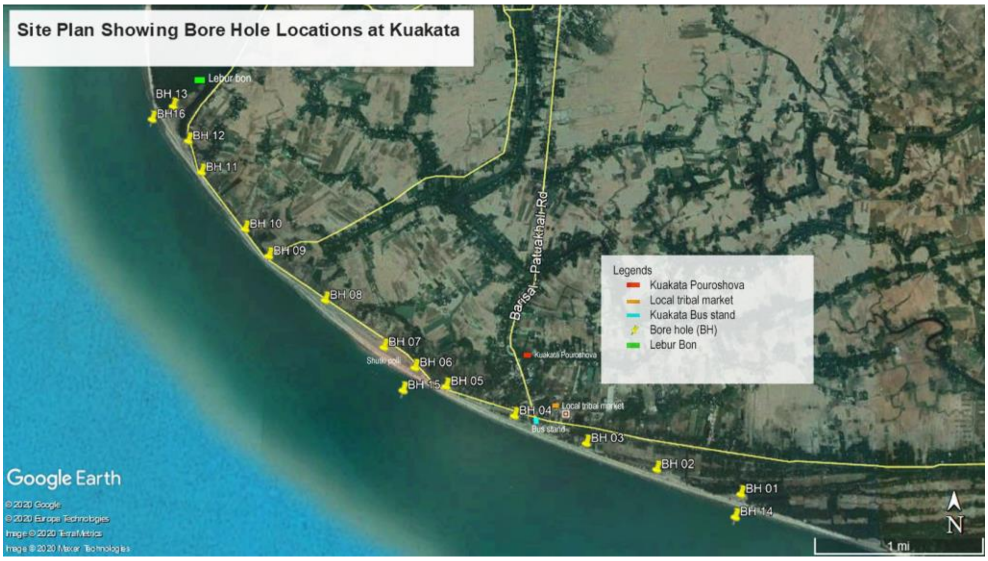

Figure 2-5 Satellite image showing the location of boreholes extracted in the 2020 geological survey. Illustration taken from ref. /1/.

3 Methodology

Considering the type and quantity of data available it was decided to use a two-sided approach to understanding the dynamics of the considered coastline:

- Analysis of shoreline and coastal profile data to determine erosional and accretional trends as well as estimate magnitude of littoral drift.
- Littoral transport modelling to assess the morphodynamic mechanisms at play.

On one hand the historical coastline data and the two recent profile surveys were used to assess the actual changes that have occurred in the coastal morphology

- The analysis of the historical coastlines will, due to the good spatial and temporal coverage, provide a good overview of the dynamics of the coast in terms of which stretches of coast are eroding or accreting and at what rates. Additionally, the analysis will provide a good estimate of the magnitude of the littoral drift along the coast.
- The coastal profile data will supplement the coastline analysis in two ways. Firstly, the profile data will be used to confirm whether the observed shoreline changes correspond to an actual shift in the coastal profile. Secondly, the profile data can be used to determine the height of the active profile which is the main parameter needed to determine the magnitude of the littoral drift from the coastline analysis.

The other side of the approach consisted of modelling the littoral drift along the considered coast. This was done by setting up a spectral wave model to determine the nearshore wave conditions along the coast and then feeding these wave conditions into a littoral drift model. This modelling approach contributes to an understanding of the mechanisms that drive the littoral drift by determining important parameters such as the wave climate and equilibrium coastline orientations.

The models were run to simulate a recent 10-year period (2011-2020). This period was chosen based on the observation that significant changes have occurred in the coastline over the past three decades and in some locations the trends have also changed (e.g.) from eroding to accreting. Similarly large changes are expected to have occurred in the bathymetry offshore of Kuakata and the available bathymetry data is therefore unlikely to be representative of the bathymetry more than a decade ago.

To ensure that the models produced reliable results, they were both calibrated against measured data. The wave model was calibrated against measured offshore and nearshore wave conditions from the two ADCP campaigns. An attempt was made to calibrate the littoral drift model by comparing calculated littoral drift to the littoral drift estimated from the coastline analysis.

4 Site visit

A site visit was carried out on March 23'rd and 24'th 2022. The inspection was carried out by walking or driving along the length of the coast indicated in Figure 4-1 and documenting the characteristics of the stretch by taking photographs of morphological features along the way. Based on observations made during the site visit, the coast has been organized into 6 sections with increasing numbers from west to east. Below, each section is described individually.

Figure 4-1 Overview of the stretch of coast that was inspected during the site visit. Coloured lines indicate the extent of coastal sections.

4.1 Section 1

This coastal section extends from the sandy spit (west) eastward to the point where the polder embankment meets the coast (east). The flat low-lying hinterland in this section (terrain level 2-3 m above MSL) is covered by the Lebur Bon forest.

The coast consists of an unprotected sandy beach of varying width. Towards the spit (north west) the beach becomes very wide (>200 m) indicating a recent advance in the shoreline.

At the eastern end of the section there are trees standing in the beach indicating severe erosion (Figure 4-2).

Figure 4-2 Photos of the beach at the eastern end (top) and the western end (bottom) of coastal section 1.

4.2 Section 2

Section 2 covers the coast between the coastal forest Lebur Bon and Kuakata town. This coastal section consists of a sandy beach backed by the dike that encloses polder 48. Along this section the seaward side of the dike is protected by a revetment consisting of concrete blocks.

As part of the Coastal Embankment Improvement Project (CEIP), the old revetment blocks are being replaced by new ones. The blocks from the old revetment are being removed from the dike and deposited on the outer part of the intertidal beach.

Due to the fact that the dike has been constructed as straight lines and that the coastline has a curved convex shape, the width of the beach between the shoreline and the dike varies considerably along this stretch of coast. In some locations the beach is thus more than 100 m wide while in other locations the general shoreline retreat has resulted in there not being any dry beach left in front of the revetment (Figure 4-3). At these locations signs of failure are seen at the foot of the revetment as blocks have fallen out from the remaining structure. It is noted that some of these blocks are dated as late as November 2019 which illustrates how quickly this failure has happened.

Figure 4-3 Photos showing the beach and revetment along section 2. Note that the photos were taken close to low tide.

4.3 Section 3

This section covers the 1300 m long stretch of coast located in front of Kuakata town and is characterized by being partly protected by geotextile bags placed on different parts of the coastal profile. At the back of the beach a large number of smaller (1-2 m) bags have been placed as revetments protecting the beachfront houses.

Additionally, large geotextile bags have been placed near the low tide level to act as breakwaters (Figure 4-4). Most of these bags showed signs of failure such as holes and sagging due to loss of sand content. Supposedly, these bags were placed in the beginning of 2022 which illustrates the limited durability of geotextile bags when used in the surf zone.

Figure 4-4 Photo showing geotextile bags on the beach at section 3.

4.4 Section 4

Section 4 covers the 3.5 km long stretch of coast just east of Kuakata town. The coast consists of a gently sloping natural beach without structures but interrupted by the outflows of two small streams. The backshore consists of low-lying forest (Figure 4-5). Some parts of the section show signs of erosion in the form of a low scarp at the landward limit of the beach or fallen trees.

Figure 4-5 Photo showing the beach at section 4.

4.5 Section 5

Section 5 covers the 1.5 km long stretch of coast located just west of the Gangamati River. Along this stretch, the shoreface consists of a sandy beach with no coastal structures but with large mudbanks protruding from the beach (Figure 4-6). The mudbanks consist of hard consolidated mud. Furthermore, dead or dying trees are found across the width of the beach. Both the exposed mud banks and the dead trees suggest severe ongoing erosion.

Figure 4-6 Photo showing the beach at section 5.

4.6 Section 6

Section 6 covers the 7.5 km long coastal stretch extending eastward from the Gangamati river. The coast consists of a natural sandy beach backed by low forested dunes. The width of the beach varies greatly due to large undulations in the shoreline. At the locations where the beach is narrow signs of erosion are seen in the form of trees that have fallen over and scarps at the top of the beach.

Figure 4-7 Photos of the beach at section 6.

5 Analysis of morphological evolution

5.1 Shoreline evolution

The evolution of the coastline over the past 30 years has been carefully analysed by comparing the available historical coastline positions. These observed changes in coastline position were then used to obtain estimates of the historical littoral drift along the coast.

In order to define the extent and orientation of the coastline to be analysed, a baseline was defined as shown in Figure 5-1. The orthogonal distance from the baseline to the coastline was then calculated for each of the historical coastlines. As shown in Figure 5-2 the shoreline positions show large displacements both on yearly and decadal timescales. Furthermore, the historical evolution varies greatly between different sections of the coast.

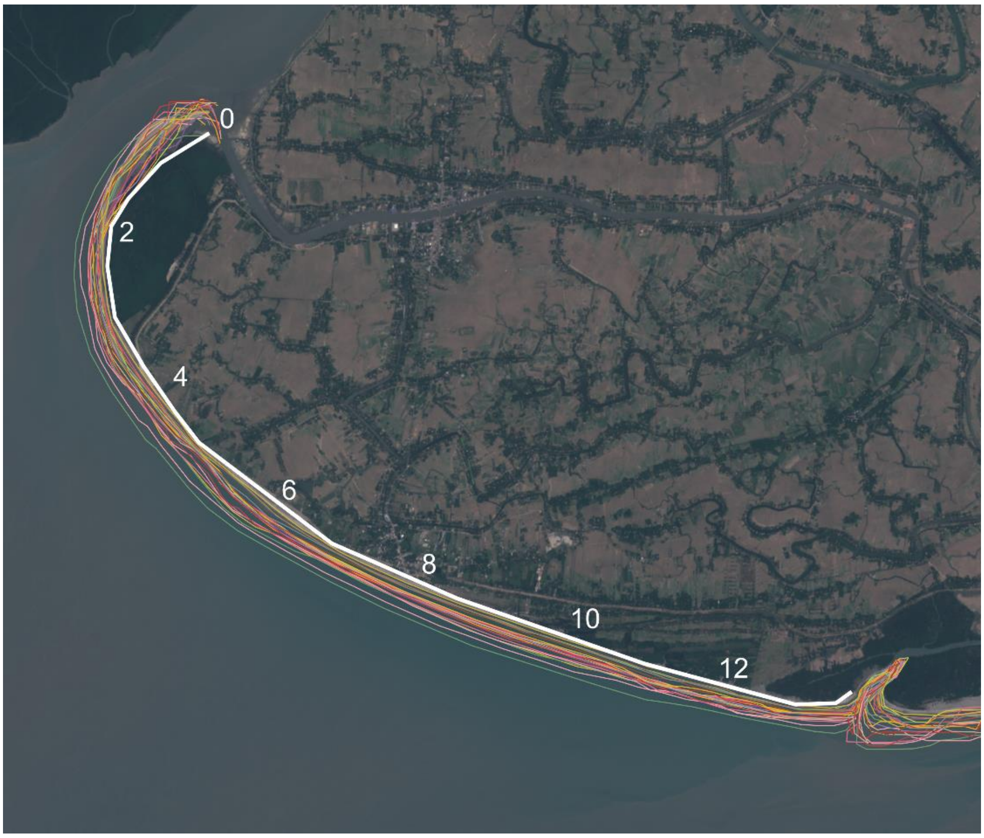

Figure 5-1 Satellite image showing the positions of historical shorelines as well as the baseline (white) used to perform the historical shoreline analysis. Numbers indicate distance (in km) along the baseline. Image credit: Modified Copernicus Sentinel data 2022/Sentinel Hub

The historical coastline positions show quite large inter-annual variations in the period 2000-2010. These displacements are due to the relatively large tides causing the water line to shift and do not reflect a displacement of the coastal profile. However, when considering shoreline changes over longer periods such as one decade, these tidal effects are averaged out and observed changes in the shoreline position can therefore be expected to provide a good description of the coastal profiles. The analysis of historical coastlines was therefore done on a decadal scale i.e. by comparing the four coastlines from 1990, 2000, 2010 and 2020 (Figure 5-3).

The analysis shows that most of the considered coastline (km 2-14) has been steadily eroding during the past 30 years at rates that typically lie in the range 10-20 m/year. On the other hand, the westernmost part of the coastline (km 0-2) has experienced a change in trend from rapid erosion in the two first decades to rapid accretion in the last decade.

Figure 5-2 Historical coastline positions at 3 locations along the coast. Shoreline position indicates the orthogonal distance from the baseline to the water line (positive in the offshore direction).

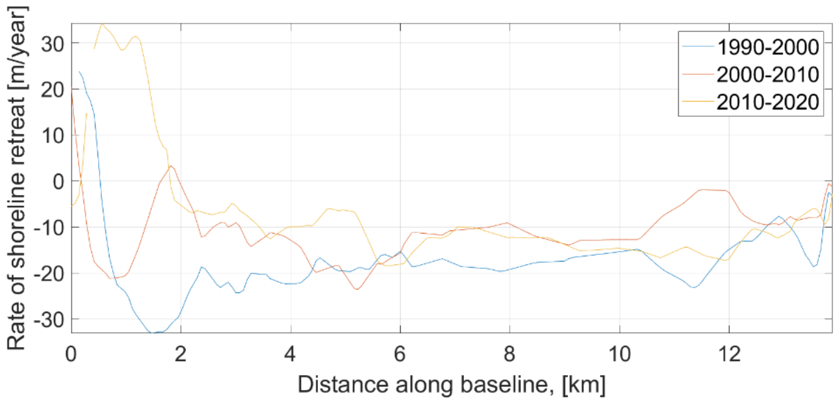

Figure 5-3 10-year average rates of change in coastline position. Positive values indicate shoreline advance.

The observed shoreline changes can be used to obtain a rough estimate of the littoral drift. To do so, it is assumed that the coastal profile at any given location maintains its shape and simply shifts in the cross-shore direction. Assuming a certain active height of the coastal profile (h_p), the alongshore gradient in the littoral drift (dq/dx) can be calculated from the rate of shoreline movement (dy/dt) using the expression:

$$\frac{dq}{dx} = h_p \frac{dy}{dt}$$

A detailed explanation of this calculation can be found in (ref /2/). The height of the active profile can be determined as the extent of the active beach above MSL plus the closure depth relative to MSL. Based on observations made during the site visit and on the available profiles the active beach is found to extend up to a level of +2 m above MSL. The closure depth was estimated both based on the wave conditions (section 6.2) and based on observed changes in the coastal profiles (section 5.2). The modelled wave conditions indicate a closure depth of 2.3-2.7 m, but due to the wave model generally underestimating the height of extreme waves this estimate is likely to be too low. The coastal profile data on the other hand suggest that the depth of closure is between -3 and -4 m MSL. Based in these observations the closure depth was set to -3.5 MSL giving an active height of the profile of 5.5 m.

In order to calculate the littoral drift along the coast it is necessary to integrate the above equation along the coast. This requires that the value of the littoral drift is known at one location on the coast. Based on littoral drift modelling (section 7) it was found that the net littoral drift is zero at x = 13 km. Using this in the integration provides the results shown in Figure 5-4.

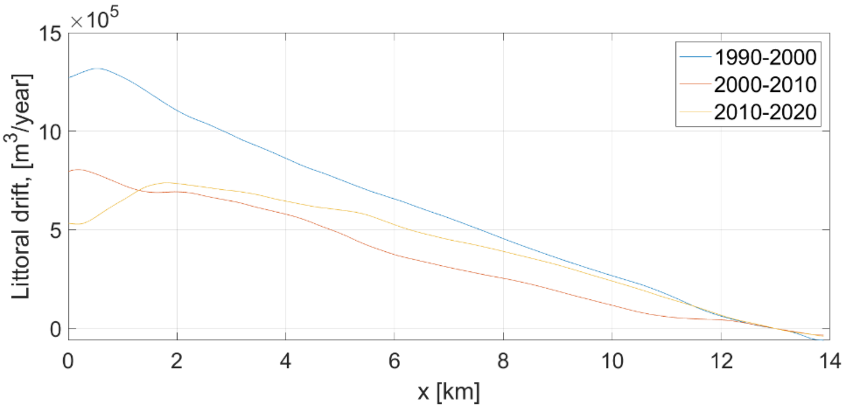

Figure 5-4 Littoral drift estimated from observed shoreline changes. Positive values indicate drift towards the west.

5.2 Profile evolution

As detailed in section 2.2, two sets of coastal profile data are available, one from 2020 and one from 2022. In this section, the general characteristics of the coastal profiles will first be described and subsequently differences between the 2020 and the 2022 dataset are analysed.

The 2020 data set is bar far the most complete of the two available data sets and is therefore used to describe the general properties of the coastal profiles. Figure 5-5 shows a typical example of one of the approximately 20km long profiles in the 2020 dataset. As seen the bathymetry south of Kuakata is quite shallow with bed levels varying between -3 m and -6 m with some large, gently sloping sand or mud banks. The westernmost profiles that are located close to the Andharmanik river show the presence of deep tidal channels leading out from the river.

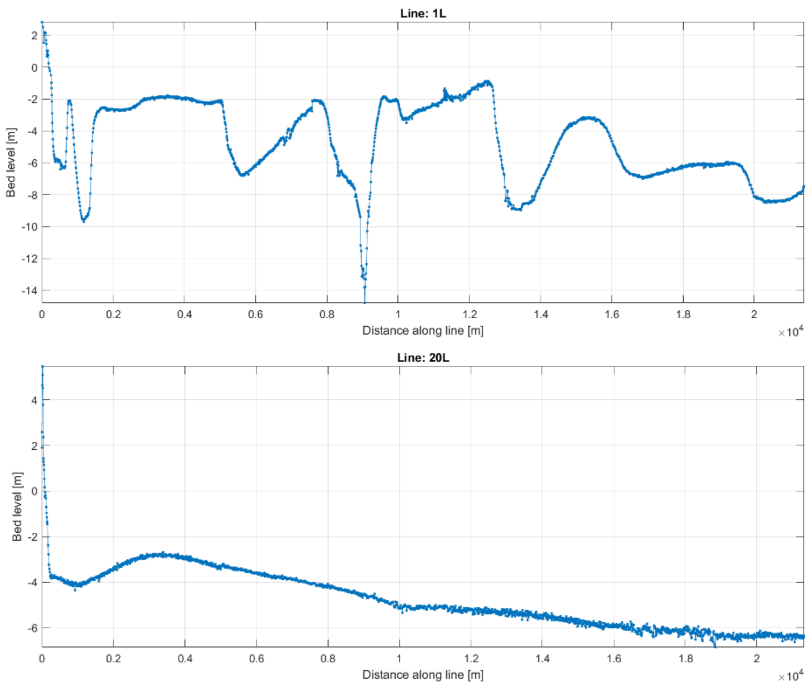

Figure 5-5 Profile plots showing the bed levels along the full length of profile 1 (top) and profile 20 (bottom) located at km 1.5 and km 5 respectively.

Plots zoomed in on the inner parts of a representative selection of the profiles measured in 2020 are shown in Figure 5-6. These profiles show that on the shoreface located at elevations between -1.5 m and 2 m, the beach is quite gently sloping with slopes generally between 1/100 and 1/50. Many of the profiles also show the presence of one or more small longshore bars. Offshore of the -1.5 m contour, many of the profiles show a steeper slope leading down to a flat plateau with a level between -3 m and -4 m. At the western end of the coastline, this plateau deepens and fades into one of the tidal channels leading into the Andharmanik river.

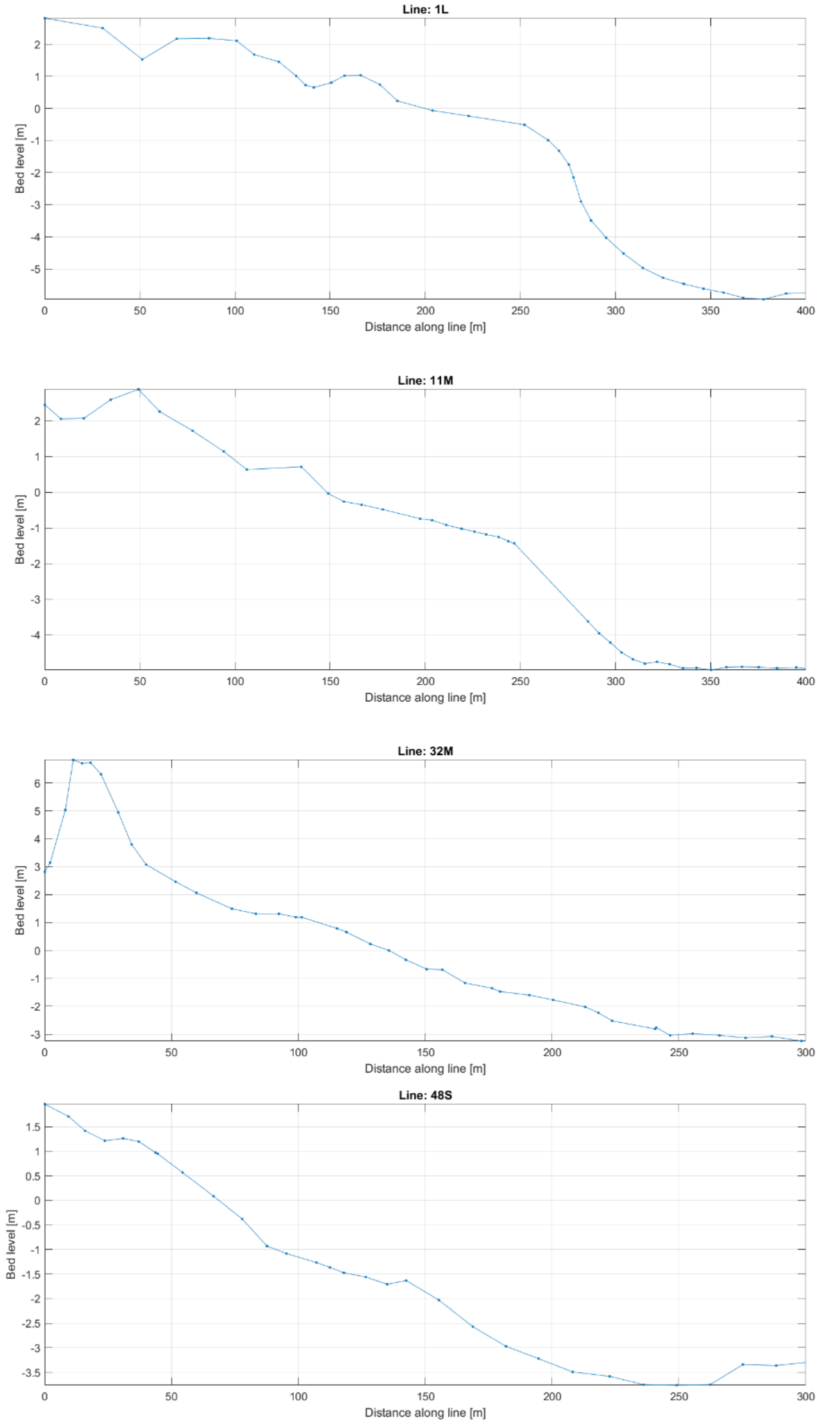

Figure 5-6 Profile plots showing the inner part of four of the profiles measured during the 2020 survey.

In order to determine possible changes in the coastal profiles a thorough comparison has been made of the data from the two surveys. Plots comparing both the geographical location of survey points as well as measured elevations for some of the profiles are shown in Figure 5-7 to Figure 5-10. Similar plots for remaining profiles are included in **Error! Reference source not found.**. The most noteworthy changes are commented below.

Most parts of profile 14 (km 3.8) have remained unchanged with the exception of the part located at elevations between -1 m and 1 m which appears to have eroded (see Figure 5-7).

In profile 20 (km 5.0) the coastal profile appears to have experienced an advance (Figure 5-8). The advance is most evident at levels between -4 m and -1 m. Some differences in the measured elevations are also seen further up in the profiles but since the part consists of revetment it seems unlikely that it would have experienced significant changes in elevation. More likely, the observed differences in terrain elevations are due to the longshore displacement between the survey points. It should be noted that profile 20 is located just east i.e. updrift (see section 7) of one of the places where concrete blocks from the old revetment have been deposited in on the beach. These old concrete blocks thus appear to have acted like a small groyne causing an updrift accumulation of sand.

At profile 26 (km 6.2) the coastal profile appears to have shifted landward at levels between -4 m and 1 m (Figure 5-9). Due to the scarcity and longshore separation of survey points it is difficult to accurately assess how far the profile has retreated but it appears to be 20-50 m. Dramatic changes have also happened higher up in the profile but these changes are most likely due to construction works on the revetment.

Profile 50 (km 11.6) has very clearly experienced a shift in the landward of 30-40 m (Figure 5-10). Similar behaviour is seen for profile 56 (km 13.1).

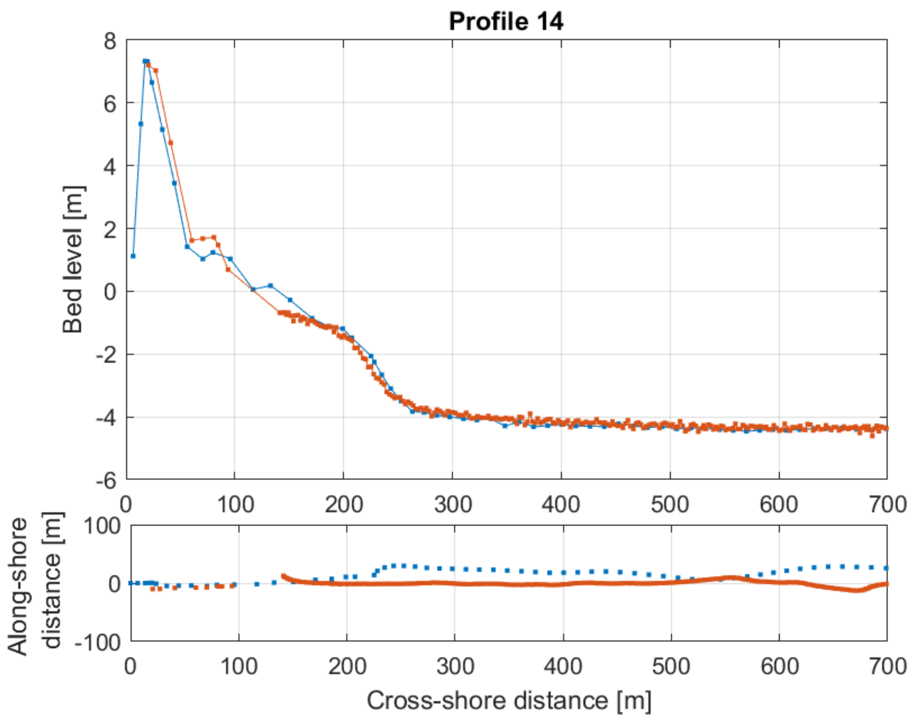

Figure 5-7 Comparison of 2020 (blue) and 2022 (red) survey data from profile 14 (3.8 km). Top: Profile view showing elevation as a function of cross shore distance. Bottom: Plan view showing longshore location as function of cross shore distance.

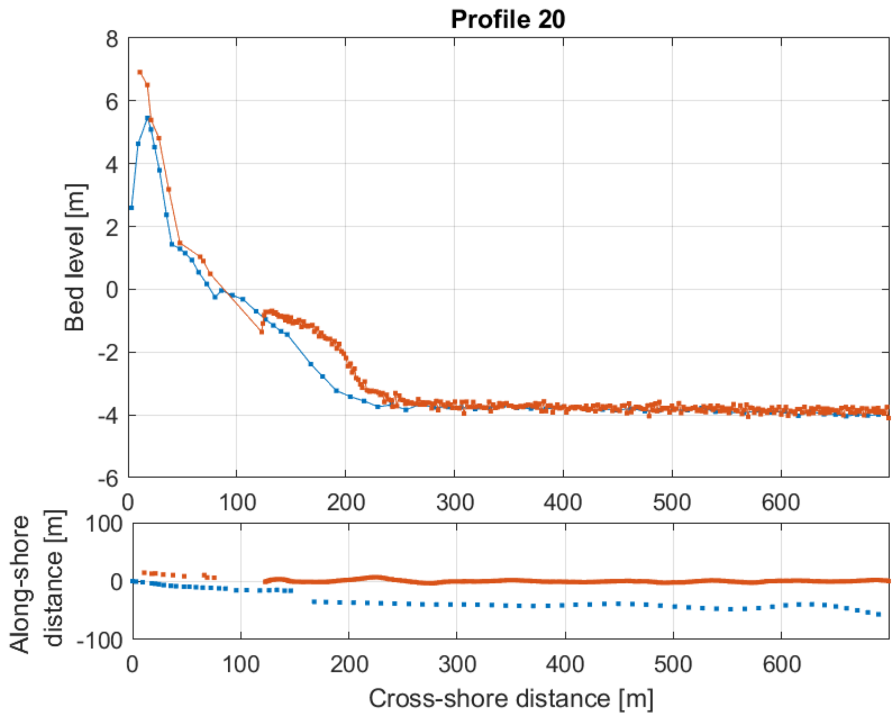

Figure 5-8 Comparison of 2020 (blue) and 2022 (red) survey data from profile 20 (5.0 km). Top: Profile view showing elevation as a function of cross shore distance. Bottom: Plan view showing longshore location as function of cross shore distance.

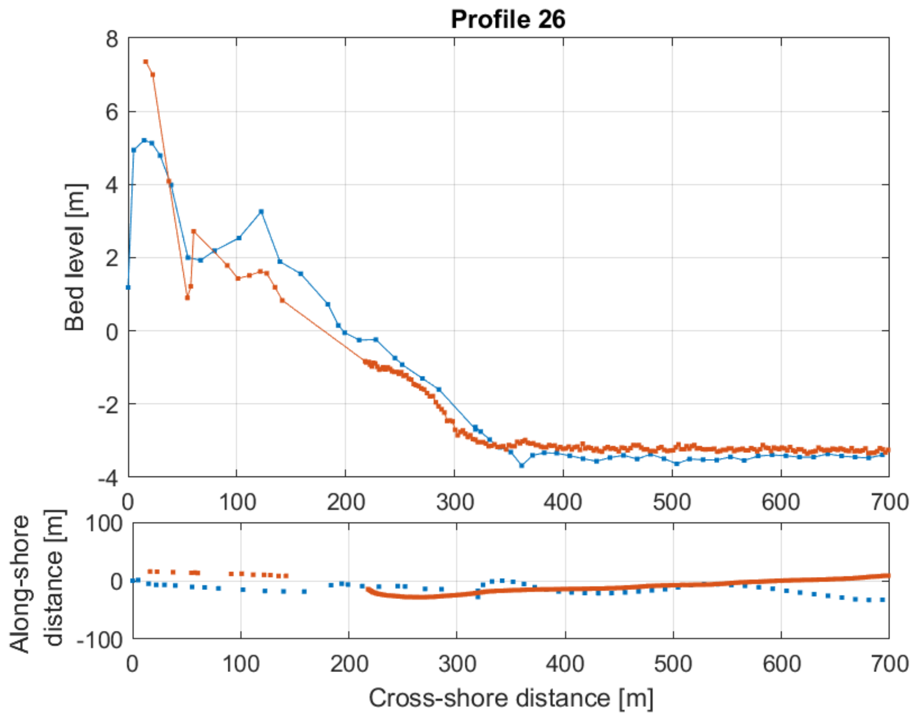

Figure 5-9 Comparison of 2020 (blue) and 2022 (red) survey data from profile 26 (6.2 km). Top: Profile view showing elevation as a function of cross shore distance. Bottom: Plan view showing longshore location as function of cross shore distance.

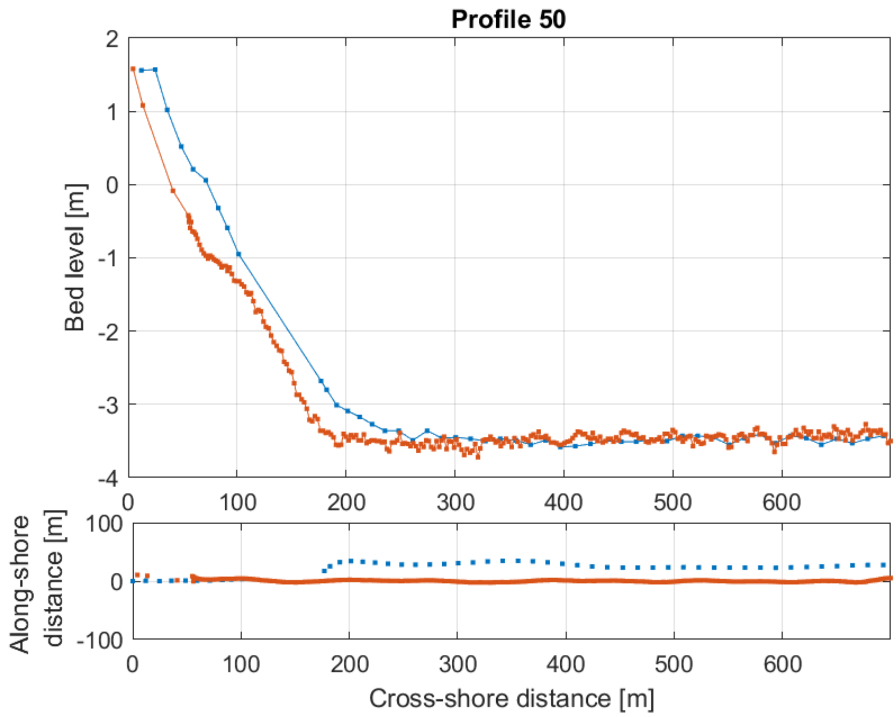

Figure 5-10 Comparison of 2020 (blue) and 2022 (red) survey data from profile 50 (11.6 km). Top: Profile view showing elevation as a function of cross shore distance. Bottom: Plan view showing longshore location as function of cross shore distance.

6 Spectral wave modelling

6.1 Model description

To assess the wave conditions at Kuakata and to provide input for littoral drift modelling, a spectral wave model was set up using MIKE 21 SW. The model domain covers the northern part of the Bay of Bengal and has one open boundary located approximately at the 16’th latitude (Figure 6-1).

An unstructured mesh made up of triangular cells was used in order to allow for a varying cell size across the model domain. Cell sizes thus varied from 40 km in the deep offshore areas to 400 m in the nearshore area around Kuakata (Figure 6-2).

The spectral wave model was run for the 10-year period from 1st of January 2011 to 31st of December 2020.

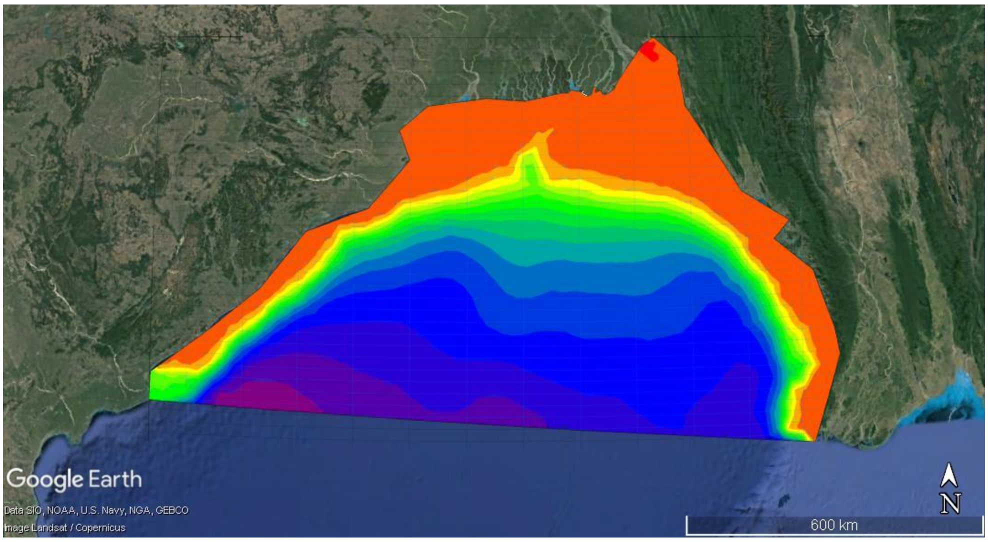

Figure 6-1 Bathymetry plot showing the extent of the model domain used for the spectral wave model.

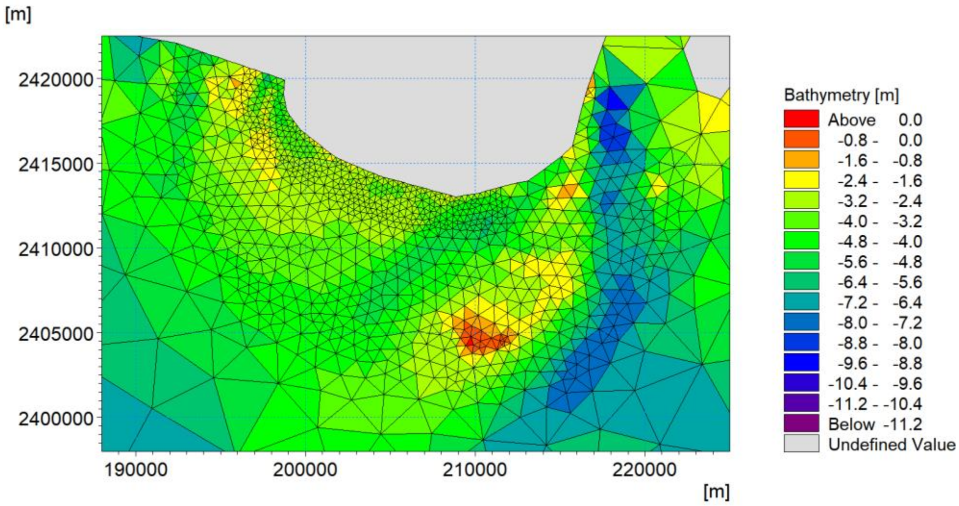

Figure 6-2 Plot of the mesh used for the SW model showing the mesh resolution in the area around Kuakata.

The spectral waves model was forced both by wind and boundary conditions. Data for both wind and wave boundary conditions were obtained from the ERA5 dataset produced by ECMWF (ref /3/). This reanalysed hindcast data provides hourly wave data with a spatial resolution of 0.5 degrees and hourly wind data with a resolution of 0.25 degrees.

The wave conditions at Kuakata are significantly affected by variations in water level. These water level variations are can be decomposed into a tidal component and a seasonal component (Figure 6-3). Tides at Kuakata are semi diurnal with spring tidal ranges of around 2.5 m. The seasonal variation causes the water level to be around 50 cm higher during the northern hemisphere summer than in the winter.

In order to represent the effect of water level variations in the model a time series of water levels at Kuakata was synthesized by adding time series of tidal variations and seasonal variations. The tidal signal was obtained using the tide prediction tool in MIKE ZERO. The seasonal variation was determined by applying a 30-day low-pass filter to the water level measurements available from Ratnabad.

A complete list of settings applied to the spectral wave model is given in Table 6-1.

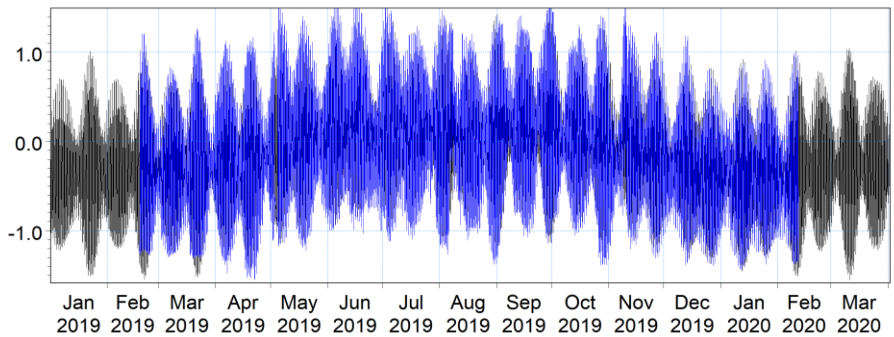

Figure 6-3 Comparison of measured water levels at Ratnabad outfall (blue) and synthesized water levels at Kuakata (black).

Table 6-1 List of settings for the MIKE 21 spectral wave model

Setting	Value
Basic equations	Fully spectral formulation Instationary formulation
Water level conditions	Varying in time, constant in domain (synthesized time-series)
Current conditions	No current variation
Wind conditions	Varying in time and domain (data from ECMWF)
Energy transfer	Quadruplet wave-wave interactions
Wave breaking	Default
Bottom friction	Nikuradse roughness length 5 cm in deeper areas (bed level below -6.5 m MSL) 1 mm in shallow areas (bed level above -6.5 m MSL)
White capping	Cdis = 2, DELTA dis = 0.5

The model was calibrated by comparing modelled wave heights and periods to measurements from the two ADCP deployments in 2018 and 2020. Calibration was mainly done by adjusting the bed roughness and the parameters controlling white capping.

As shown in Figure 6-4 and Figure 6-5 the model performs reasonably well in terms of reproducing the measured significant wave heights and peak wave periods. Unfortunately, the wave conditions were generally quite gentle during the two ADCP campaigns and therefore the available data does not provide an opportunity to calibrate or validate the model in very energetic conditions. Both the 2018 and the 2020 datasets show a few short peaks in the measured wave heights and the model generally tends to underestimate the wave height during these events. All of these events are caused by short periods of strong local winds from W or NW directions. The discrepancy between modelled and measured wave heights during these events is therefore expected to be due to the applied wind fields not resolving the local winds properly.

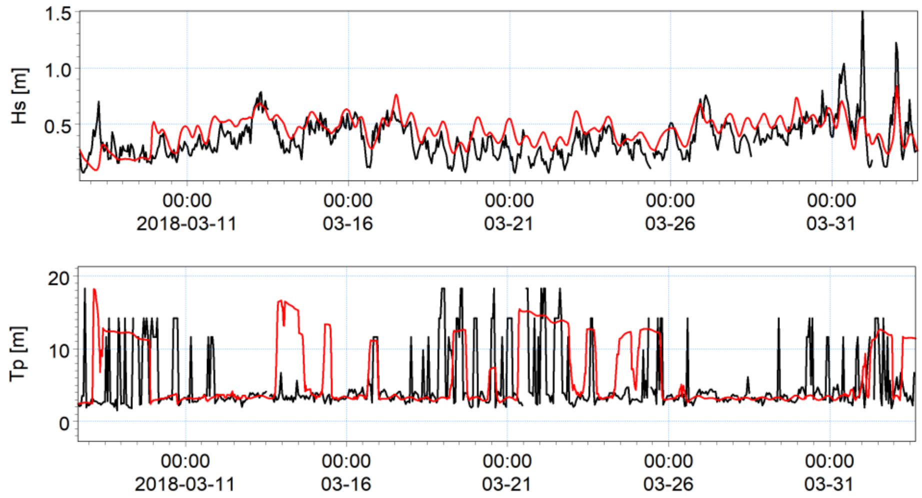

Figure 6-4 Time series plots comparing modelled (red) and measured (black) wave parameters during the 2018 offshore ADCP deployment.

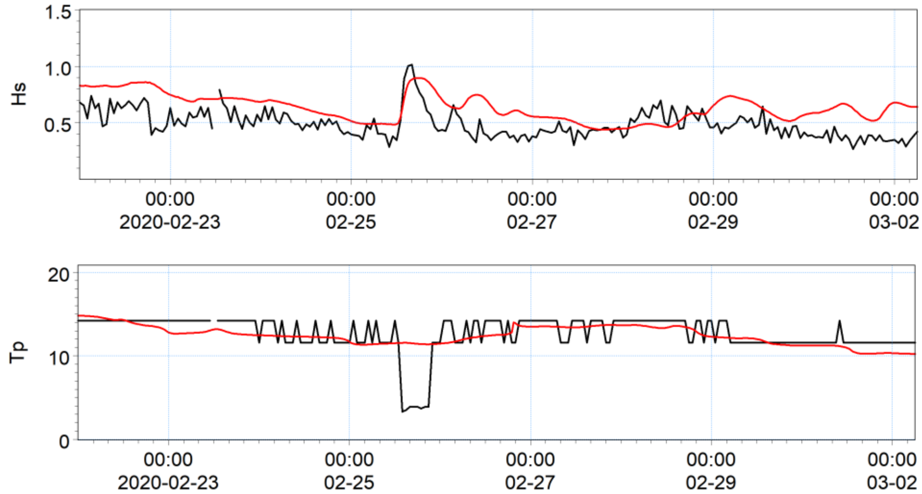

Figure 6-5 Time series plots comparing modelled (red) and measured (black) wave parameters for the 2020 offshore ADCP deployment.

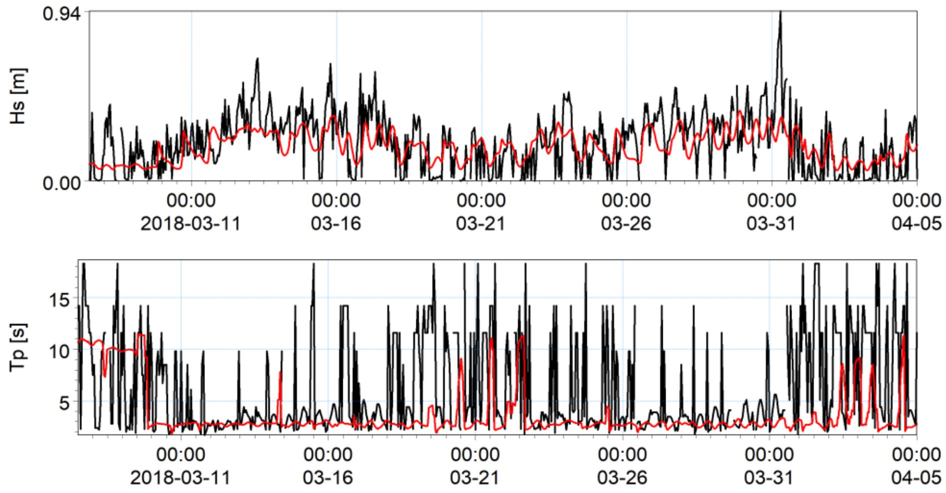

Figure 6-6 Time series plots comparing modelled (red) and measured (black) wave parameters for the 2018 nearshore ADCP deployment.

Looking at the calibration at the 2018 nearshore ADCP (Figure 6-6) it is seen that the model performs reasonably well although there are significant differences between modelled and measured values. The measured wave heights vary quite rapidly (faster than the 12-hour tidal period) compared to the modelled wave height. The modelled wave heights show much less short-term variation although the longer term trends are reproduced fairly well. It is noted that the model underpredicts the wave height during more energetic conditions.

6.2 Results

In order to provide input data for the littoral drift modelling, timeseries of wave parameters have been extracted in 7 points along the considered coast namely at the location of profiles 1, 6, 10, 23, 34, 45 and 56 (see locations in Figure 6-7). The extraction points were placed on the flat plateau in the coastal profile 100-200 m from the shoreline.

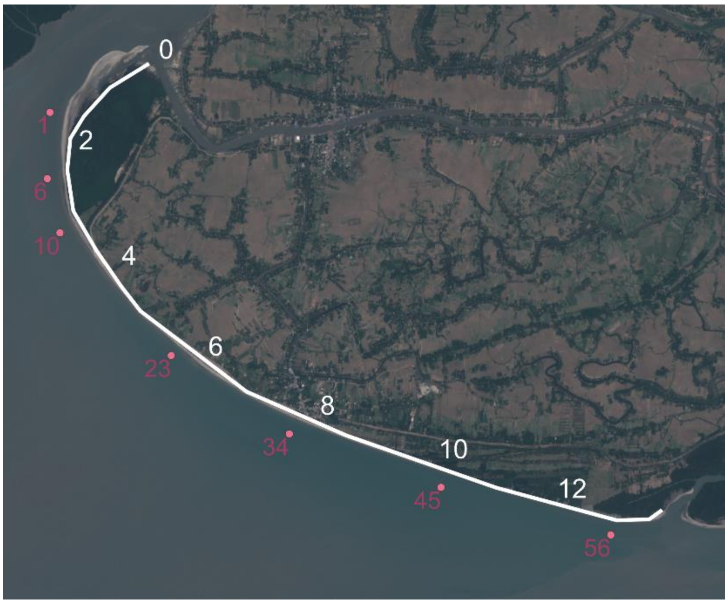

Figure 6-7 Satellite image showing the locations of profiles (pink dots) where wave conditions were extracted and littoral drift calculations were performed. White numbers indicate distance along baseline in km. Image credit: Modified Copernicus Sentinel data 2022/Sentinel Hub

As shown in Figure 6-8 the wave climate at Kuakata is very mild and the significant wave height only very rarely exceeds 1 m (Figure 6-8). This is to a large degree due to the very shallow bathymetry offshore of Kuakata which causes most of the wave energy to be dissipated over the last 50 km before they reach the shore.

Due to the relatively smooth shape of the coastline combined with the absence of dramatic features in the nearby bathymetry, the wave conditions only vary gradually along the coast. As shown in Figure 6-8, waves approach Kuakata from a narrow range of directions around SSW. Wave heights are generally highest in the central part of the coastline. At the western end, the coastline orientation means that the coast is sheltered from easterly waves and refraction reduces the height of incoming waves. On the other hand, the eastern end is slightly sheltered by offshore shoals and islands (Figure 6-2).

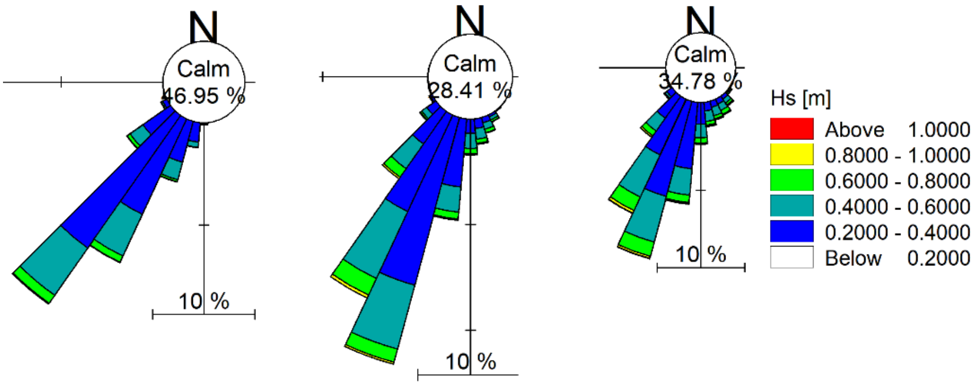

Figure 6-8 Wave roses showing the modelled wave conditions at points a (left), b (centre) and c (right).

A characteristic feature of the wave climate at Kuakata is that it consists of distinctly defined swell and wind sea components. The swell waves originate in the southern Indian Ocean and arrive at Kuakata as very small amplitude (H_s typically 0.1-0.2 m) and long wave periods (T_p typically between 10 s and 15 s). The wind sea waves on the other hand are typically generated in the northern part of the Bay of Bengal and typically have larger wave heights (Hs around 0.5 m) and short wave periods (T_p around 3 s).

An important parameter when studying coastline evolution is the depth of closure (d_l) and an estimate of this value can be obtained from the nearshore wave conditions using the equation (Ref. /4/):

$$d_l = 2.28\, H_{s,12} - 68.5\, \frac{H_{s,12}^2}{gT_{p,12}^2}$$

Where $H_{s,12}$ is the significant wave height exceeded 12 hours per year, $T_{p,12}$ is the corresponding wave period and g is the acceleration of gravity. Calculated depths of closure are listed in Table . It should be noted that, since the present spectral wave model is found to underestimate wave heights during energetic events, the present calculation of closure depths most likely results in too shallow a closure depth.

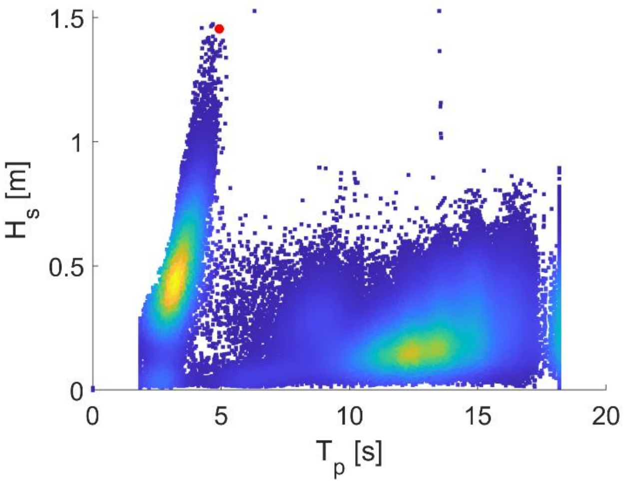

Figure 6-9 Scatterplot showing modelled significant wave heights and peak wave periods at the location of profile 34 (km 7.8). The red dot indicates the wave height ($H_{s,12}$) and period ($T_{p,12}$) exceeded 12 hours a year.

7 Littoral drift modelling

7.1 Model description

The littoral drift along the considered coast has been simulated by application of the littoral drift model in the LITPACK software package. This model (commonly referred to as LITDRIFT) simulates waves, hydrodynamics and sediment transport close to shore. Based on the shape of the coastal profile, the wave conditions and water level conditions at the offshore end of the coastal profile the LITDRIFT model calculates:

- The changes to the waves as they propagate towards shore including the effects of shoaling, refraction, bed friction, wave breaking and water level variations.
- The longshore current and water level variations due to effects of wave radiation stresses, tides and bed friction.
- Longshore sand transport due to the combined action of waves and currents.

LITDRIFT simulations were performed at 7 the locations indicated in Figure 6-7.

To represent the effect of varying water levels on the littoral drift, all simulations were run using the same time-series for water levels as was used in the spectral wave model.

A key parameter in the LITDRIFT model is the roughness of the seabed. Bed roughness provides a resisting force against the longshore current and increasing the bed roughness therefore reduces the magnitude of the littoral drift. Because the bed roughness is generally not known it is normally used as a calibration parameter to ensure that the magnitude of the simulated littoral drift matches estimates from other sources (e.g. coastline analysis).

In an attempt to calibrate the presently developed LITDRIFT model, the littoral drift at profile 23 (km 5.6) has been simulated using a range of values for the bed roughness. In this setup, the bed roughness is described by a Nikuradse roughness length which has been varied between 0.01 mm and 10 mm. This range was selected based on the consideration that, for sandy beaches without ripples, the bed roughness length should be around 2.5 times the median grain size. At the considered site the median grain size is consistently around 0.11 mm leading to an expected bed roughness of about 0.28 mm.

Results of the sensitivity test are shown in Figure 7-1. These results should be compared with the results of the shoreline analysis which estimated the littoral drift at the same location to be around 600,000 m^3/year (see Figure 5-4, km 5.6). The results of the sensitivity test show that even the lowest roughness length considered gives a modelled littoral drift that is less than 1/3 of the drift estimated in the shoreline analysis. Considering that the smallest simulated roughness length is already about 30 times smaller than the roughness length expected based on the sediment grain size the discrepancy between modelled and observed littoral drift is expected to be due to other factors than the bed roughness. Rather than trying to compensate for these factors by using a very unrealistic roughness length it was chosen to use a more realistic roughness length of 0.1 mm. The other factors leading to the discrepancy between modelled and observed littoral drift are discussed in section 8.

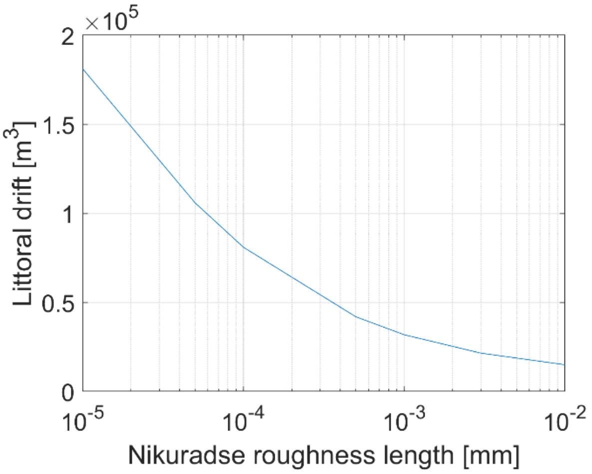

Figure 7-1 Effect of varying bed roughness on littoral drift calculated for profile 23 (one-year period in 2016).

7.2 Results

Results of the present littoral drift modelling are summarised in Table .

Table 7-1 Summary of the results from the LITDRIFT modelling

Profile #	Km	$H_{s,12}$ [m]	$T_{p,12}$ [s]	Closure depth [m]	Coastline Orientation [degrees]	Equilibrium Orientation [degrees]	Net drift [m^3/year]	Gross drift [m^3/year]
1	1.5	1.2	5.1	2.3	280	215	74,000	74,000
6	2.3	1.2	5.2	2.4	263	210	103,000	103,000
10	3.1	1.3	5.1	2.4	247	206	120,000	121,000
23	5.6	1.2	5.2	2.4	222	203	99,000	105,000
34	7.8	1.2	5.0	2.4	203	193	55,000	83,000
45	10.3	1.2	13.5	2.7	197	193	34,000	97,000
56	13.1	1.5	4.9	2.7	190	191	-9,000	118,000

7.2.1 Direction of littoral drift

Overall, the littoral drift modelling indicates that, on almost the entire considered coast, the littoral drift is directed towards west. Only at the very eastern end (profile 56) is the transport directed towards east. This is due to the curved shape of the coastline close to the outflow of the Gangamati river.

For each of the 7 profiles Q-alpha curves have been determined by calculating the littoral drift for a range of coastline orientations around the actual coastline orientation (Figure 7-2). These Q-alpha curves have also been used to determine the equilibrium orientation of the coast i.e. the orientation of the coast that would cause the net littoral drift to be zero.

Results show that the equilibrium orientation only varies slightly along the coastline from 191 degrees at the eastern end to 215 degrees in the western end. The large longshore variations in the modelled littoral drift are therefore mainly due to the variations in coastline orientation which cause the difference between equilibrium orientation and coastline orientation to increase towards the west. Thus, at km 13 the coastline orientation is equal to the equilibrium orientation causing the net littoral drift to be close to zero. Near profile 6 (km 2.3) the difference between the equilibrium orientation and the coastline orientation is approximately 50 degrees which means that the littoral drift is the largest it can be for this wave climate. Even further west, at profile 1 (km 1.5), the difference between the equilibrium orientation and the coastline orientation increases to approximately 65 degrees resulting in a smaller littoral drift.

In summary, the LITDRIFT modelling indicates a westward littoral drift that increases from km 13 to km 2.3 and then decreases west of km 2.3. Consequently, the modelling suggests that the coast between km 2.3 and km 13 should be eroding and that the coast west of km 2.3 should be accreting. This is in qualitative agreement with the result of the analysis of the coastline changes during the modelled period (Figure 5-4).

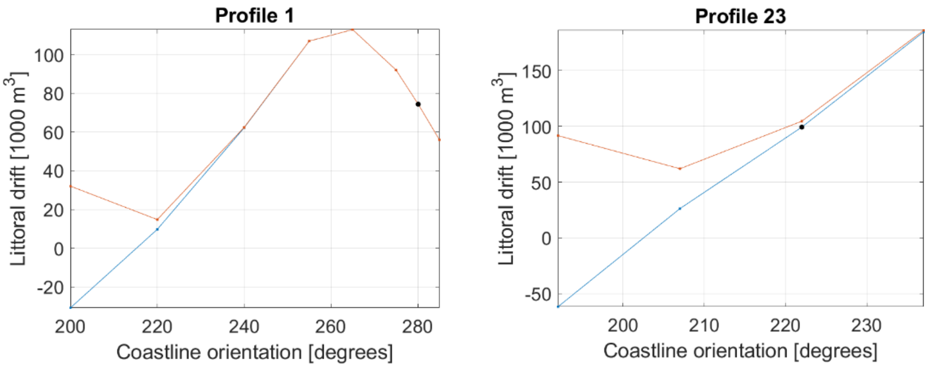

Figure 7-2 Examples of Q-alpha curves showing how the net (blue lines) and gross (red lines) littoral drift varies with coastline orientation. Black dots indicate the present coastline orientations.

7.2.2 Temporal variation

The fact that the littoral drift has been simulated for a period of 10 years make it possible to evaluate the temporal variations both between seasons and between years.

With regards to the seasonal variations, the modelling shows that the large majority of the littoral drift occurs in the northern hemisphere summer as wave heights are generally very calm in the northern hemisphere winter.

For the eastern part of the coast where the difference between coastline orientation and equilibrium orientation is relatively small the results also show a clear seasonal variation in direction of the littoral drift. Thus, during the the first half of the year the littoral drift is mostly directed towards the east (negative values) while in the last half of the year the transport is mostly directed towards the west (positive values).

Furthermore, the eastern part of the coast also experiences a large inter-annual variation in both the net and gross littoral drift. This variation appears to be caused not so much by variations in wave height but by variations in wave directions. To illustrate the importance of interannual variations it is noted that at profile 45 (km 10.3) the average net annual littoral drift is 34.000 m^3 but the maximum and minimum annual littoral drifts are 93,000 m^3 and -2,000 m^3 respectively.

Further towards the west, the characteristics of the littoral drift changes significantly mainly due to the fact that the coastline orientations deviate more and more from the equilibrium orientation. As a result, the westerly-directed net littoral drift increases and the inter-annual variation in littoral drift becomes smaller. Thus, at profile 10 (km 3.1) the maximum and minimum annual littoral drift only deviate by about 20 % from the average value of 120,000 m^3.

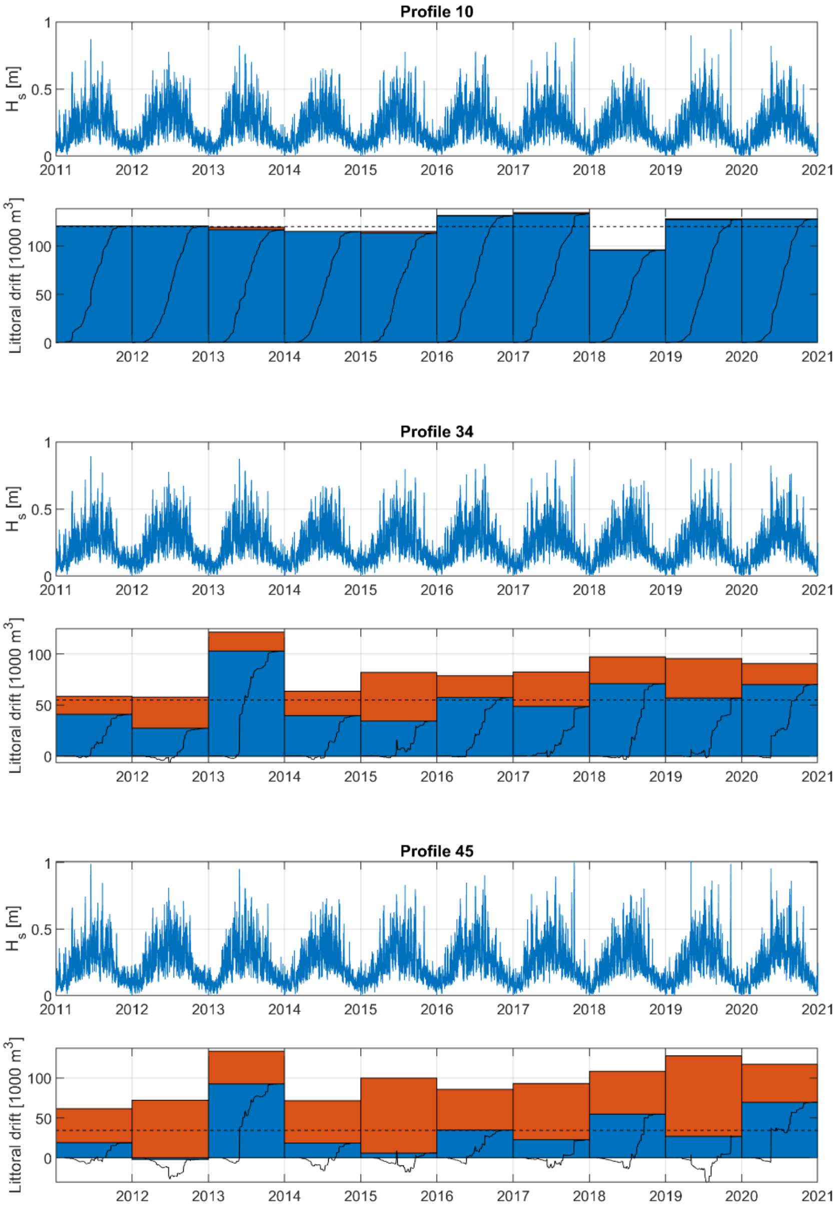

Figure 7-3 Overview of the temporal variation in littoral drift. For each profile the top panel shows the significant wave height and the bottom panel shows the littoral drift. Littoral drift is illustrated as a time-series of yearly accumulated net transport (black lines), yearly gross (red bars) and net (blue bars) littoral drift.

7.2.3 Distribution of littoral drift in the coastal profile

Because the LITDRIFT model calculates the longshore sediment transport in all parts of the coastal profile it can be used to assess where in the coastal profile the littoral drift occurs. As shown in Figure 7-4, almost all of the littoral drift occurs at elevations between -1 m and +1 m MSL. According to the LITDRIFT model, longshore transport occurs out to slightly beyond the -2 m depth contour. This is in good agreement with the calculated closure depth which for this profile (23) is 2.4 m.

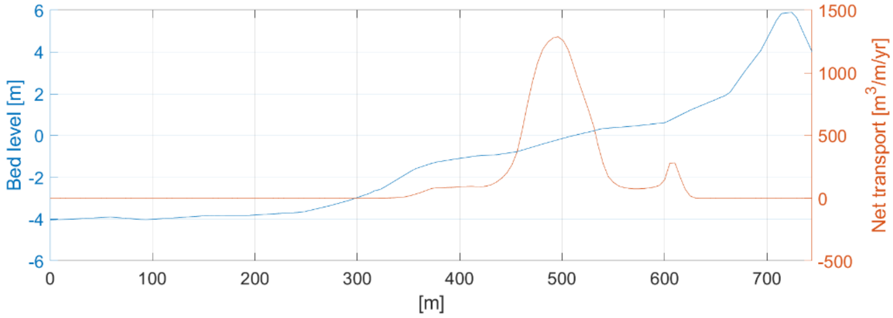

Figure 7-4 Profile plot showing the bed level and calculated net littoral drift in profile 23 (km 5.6).

8 Discussion

8.1 Summary of findings

In the present project a large amount of information regarding the Kuakata coast has been compiled and analysed. Additionally, detailed numerical models have been set up describing the wave conditions and longshore sediment transport along the coast. This has provided valuable new insights regarding the coastal dynamics. Some of the key findings are:

- With the exception of the westernmost end the entire considered coastline is eroding at rates of 10-20 m/year.
- Shoreline changes are related to a cross shore translation of the coastal profile at elevations roughly between -3.5 m and 2 m MSL.
- Based on the observed changes in shoreline positions and coastal profiles it is estimated that the littoral drift on some parts of the coastline is around 600,000 m^3/year. This is one order of magnitude larger than previous studies.
- Littoral drift modelling has shown that the littoral drift is zero just west of the Gangamati River and west of this point the littoral drift is directed towards the west. Furthermore, the magnitude of the littoral drift increases steadily towards the west until the Lebur Bon forest where the large difference between coastline orientation and equilibrium orientation causes the littoral drift to decrease.
- The parts of the coast where the littoral drift model predicts erosion/accretion match the erosion/accretion patterns found in the shoreline analysis.
- The magnitude of the modelled littoral drift is roughly a factor of 5 smaller than the littoral drift estimated from the coastline analysis.

8.2 Limitations of the present work and suggestions for further studies

A significant challenge in the present project has been to understand what causes the very large changes in the coastal morphology that have been observed over the past few decades. Considering the very gentle wave climate at Kuakata, the 600,000 m^3/year estimate of the littoral drift obtained from the coastline analysis appears very large. Indeed, the present modelling of littoral drift gives results that qualitatively agree with the coastline analysis but are roughly 5 times smaller in magnitude. Attempts have been made to modify both the coastline analysis and the numerical models in order to reduce this discrepancy but as explained below this would require better input data for the wave modelling. Below, a discussion of the results is provided that can hopefully help guide future studies to obtain more consistent results.

The first result that might be questioned is the estimate of littoral drift obtained from the coastline analysis. However, considering the relative simplicity of the considered coastline such an analysis should provide a fairly good estimate of the magnitude of the littoral drift. A main uncertainty in the estimate lies in the one parameter in the calculation namely the active height of the profile which has been set to 5.5 m. This value has been chosen based on observations of measured coastal profiles. These profiles quite clearly show that the part of the coastal profile located at elevations between roughly -3.5 m and 2 m MSL have shifted in the landward direction. In order to reduce the estimate of the littoral drift it would be necessary to use a smaller value for the active height, but this does not seem to be justifiable based on the available information.

The cause for the discrepancy is more likely to be found in modelling of littoral drift which could be improved in 3 ways.

Firstly, despite the efforts made to calibrate the spectral wave model it was found that the model underestimates the wave height during some periods with relatively high waves. These periods were related to short events with strong local winds. It is therefore suspected that the observed discrepancies between modelled and measured wave heights is due to the relatively coarse resolution of the wind fields used in the present modelling. It might be possible to improve the performance of the spectral wave model by using more detailed wind fields the provide a better description of local winds. To illustrate the potential effect of improving the wave model it should be noted that the magnitude of the littoral drift roughly scales with the wave height to the power 3.5. Increasing the wave height by a factor of 1.5 should thus lead to an increase in the littoral drift of more than a factor of 4.

Another challenge when calibrating the spectral wave model has been the limited amount of measured wave data available. The available wave data covers two periods with a combined duration of approximately 1.5 months. These periods only include very few events with relatively high waves and therefore provide a rather poor data basis for calibrating a wave model. In order to be able to set up more reliable wave models in the future it is therefore measured wave conditions over a longer period of time. This time-period should cover the northern hemisphere summer as this is the season when large wave events are most likely to occur.

Secondly, the modelling could be improved by including a better representation of cyclones. The present wave modelling used wind data with a spatial resolution of 0.5 degrees which is not sufficient to ensure a proper description of cyclones. It is very likely that a better representation of cyclone winds would increase the modelled wave heights during cyclones and thereby also increase the modelled littoral drift (as described for the general wave conditions above). It is therefore recommended to do detailed modelling of wave conditions during cyclones and include these events in the littoral drift modelling.

Lastly, the present modelling does not include the effect of tidal currents on the littoral drift. At most locations, tidal currents do not have a significant effect on littoral drift, and they are therefore normally ignored when modelling littoral drift. However, in the present case where the wave climate seems to be too mild to explain the very large observed changes in the coastline it could be suspected that tidal currents have a significant effect on the littoral drift. In order to assess this effect, it would be necessary to set up a hydrodynamic model that accurately describes the tidal currents around Kuakata.

8.3 Discussion of coastal protection strategies

There is a strong need to stop the on-going shoreline retreat at the entire coastline to stop further loss of assets. The two main assets to protect are the embankment enclosing poulder 48 and buildings at Kuakata town. Secondary assets to protect are the natural areas such as Lebur Bon forest at the western end of the considered coast.

Based on the present assessment of the on-going coastal erosion it is concluded that the only protection scheme that could ensure protection of the entire coastline including Lebur Bon forest is sand nourishment. However, due to the large magnitude of the littoral drift along the coast at Kuakata such a strategy would involve very large volumes of sediment to be nourished on a regular basis and consequently pure sand nourishment is not considered a viable option to prevent further erosion.

Instead, a more suitable approach would be to use strategically placed hard coastal protection structures such as groynes. If properly designed, groynes can be very effective in stopping erosion especially on coasts where the present coastline orientation is close to the equilibrium orientation. In such cases groynes can be used to establish stable beaches that are aligned with the equilibrium orientation and thereby experience a net zero littoral drift. For this to be possible it is necessary that the groynes are long enough to prevent any sand bypass.

It should be emphasized that the numerical modelling presented in this report has shown some important discrepancies when compared to the observed shoreline changes. Thus, the littoral drift model is expected to greatly underestimate the magnitude of the littoral drift and the results of the coastline analysis should therefore be considered as the most reliable estimate. There is however more confidence in some of the results of the numerical modelling most notably the calculated equilibrium orientations.

Design of any sort of coastal protection scheme should take into account the significant uncertainties related to the present understanding of the coastal dynamics in the area.

9 References

/1/ Feasibility Study for Protection and Development of Kuakata Sea Beach (2021), Institute for water modelling, Bangladesh

/2/ Mangor, K., Drønen, N., Kærgaard, K., Kristensen, S. (2017): Shoreline Management Guidelines. DHI

/3/ Hersbach, H., Bell, B., Berrisford, P., Biavati, G., Horányi, A., Muñoz Sabater, J., Nicolas, J., Peubey, C., Radu, R., Rozum, I., Schepers, D., Simmons, A., Soci, C., Dee, D., Thépaut, J-N. (2018): ERA5 hourly data on single levels from 1959 to present. Copernicus Climate Change Service (C3S) Climate Data Store (CDS).

/4/ Hallemeyer, R. J. (1981): A profile zonation for seasonal sand beaches from wave climate. Coastal Engineering, 9, 527-544

APPENDIX A – Coastal profile plots

A Flow fields over the sandbars in the Pussur River

This appendix includes plots that compare data from the 2020 and the 2022 coastal profiling surveys.

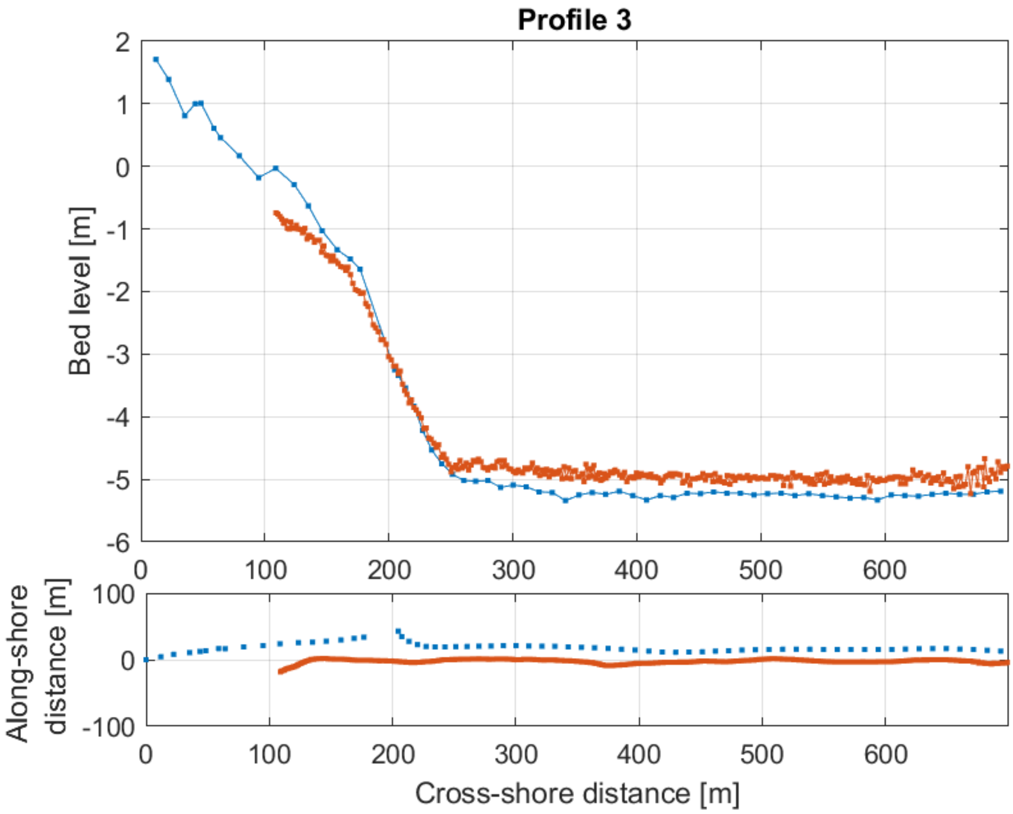

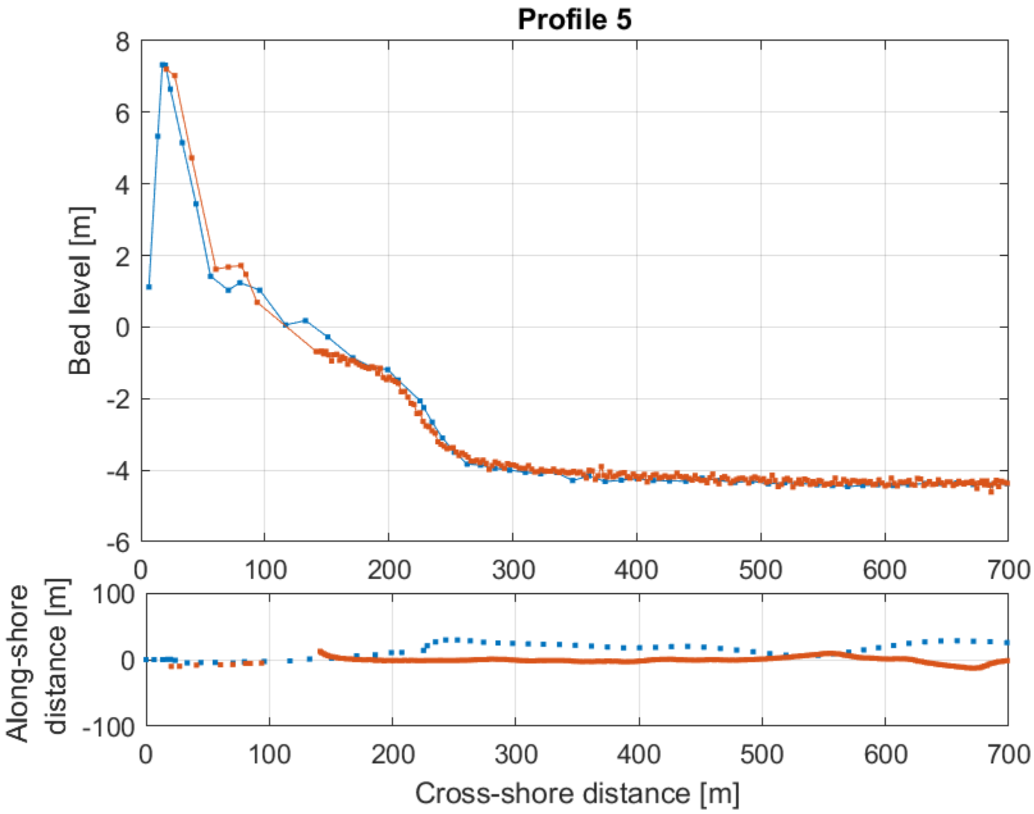
Profile 5
Bed level [m]
Along-shore distance [m]
Cross-shore distance [m]

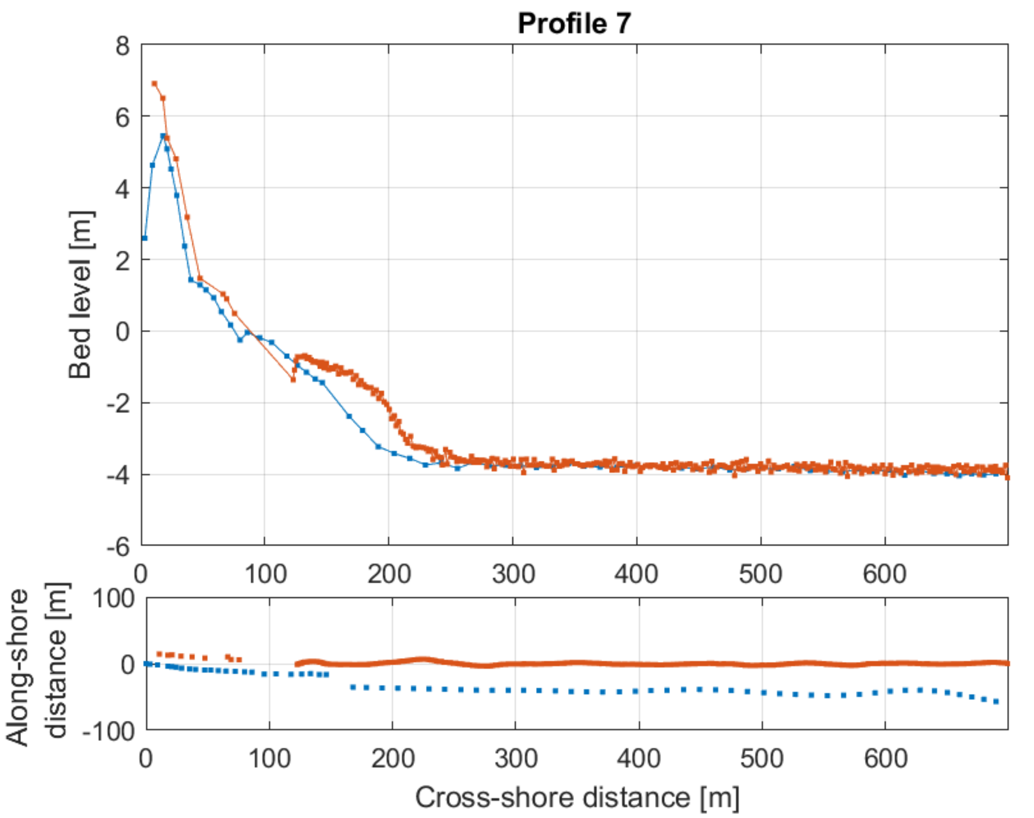
Profile 7
Bed level [m]
Along-shore distance [m]
Cross-shore distance [m]

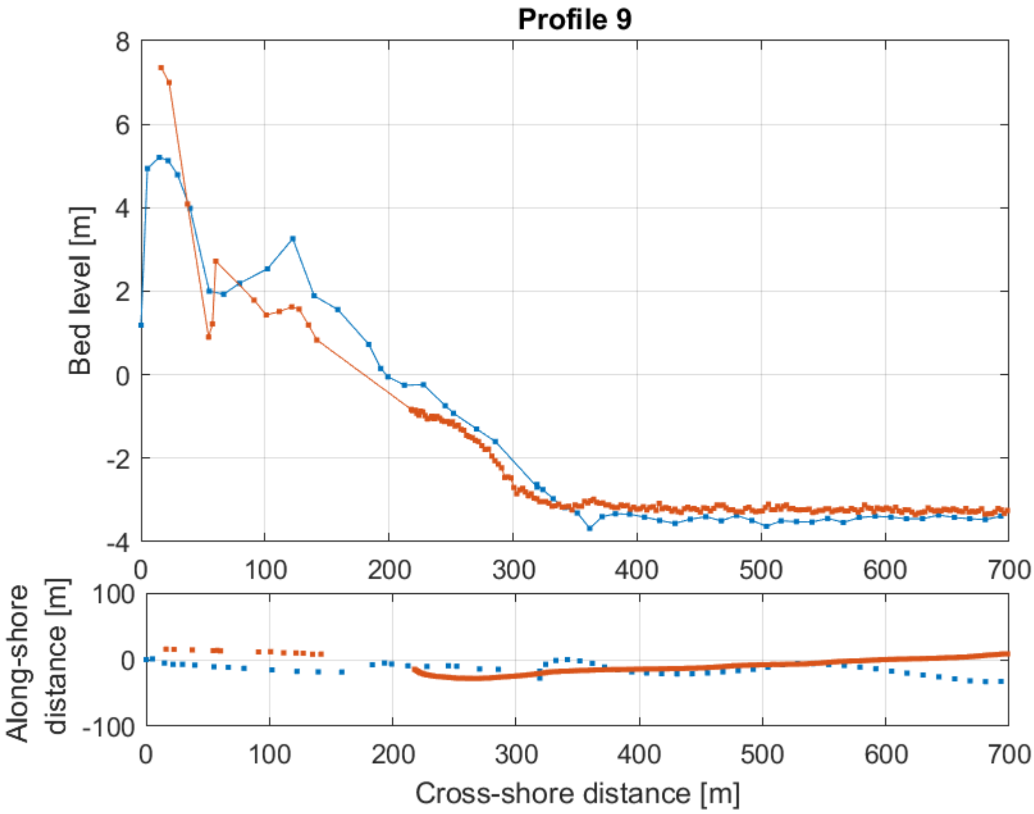
Profile 9
Bed level [m]
8
6
4
2
0
-2
-4
0
100
200
300
400
500
600
700
Along-shore distance [m]
100
0
-100
Cross-shore distance [m]

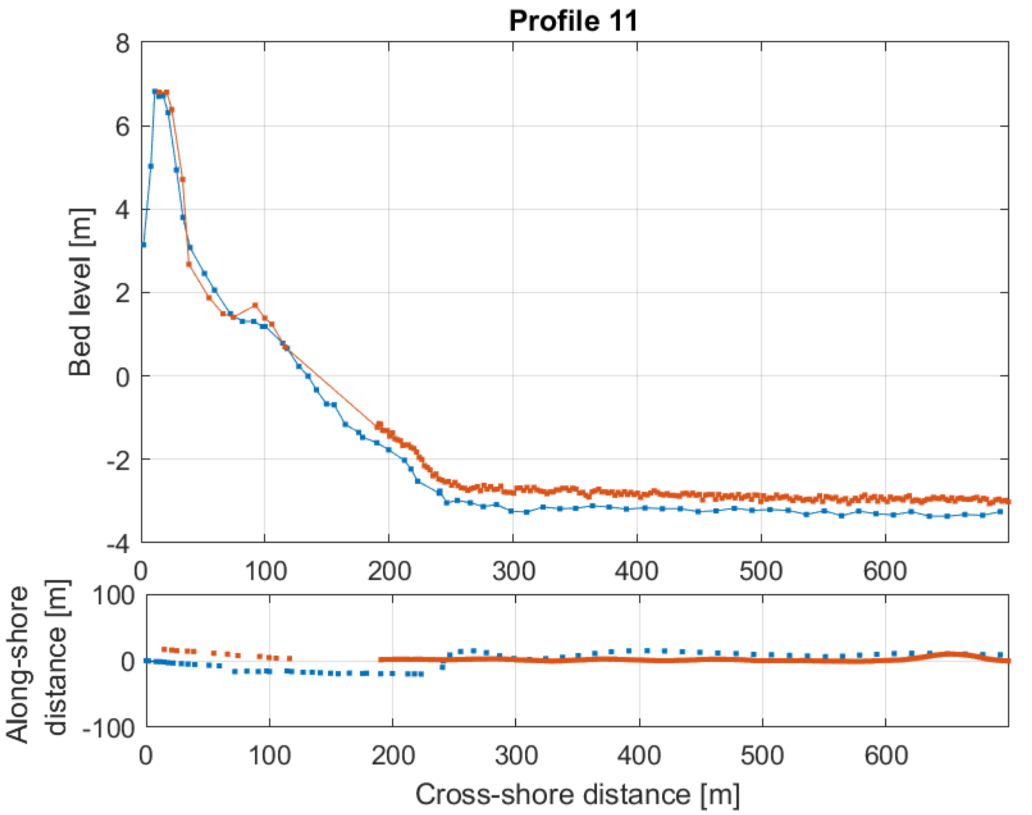
Profile 11
Bed level [m]
8
6
4
2
0
-2
-4
0
100
200
300
400
500
600
Along-shore distance [m]
100
0
-100
Cross-shore distance [m]

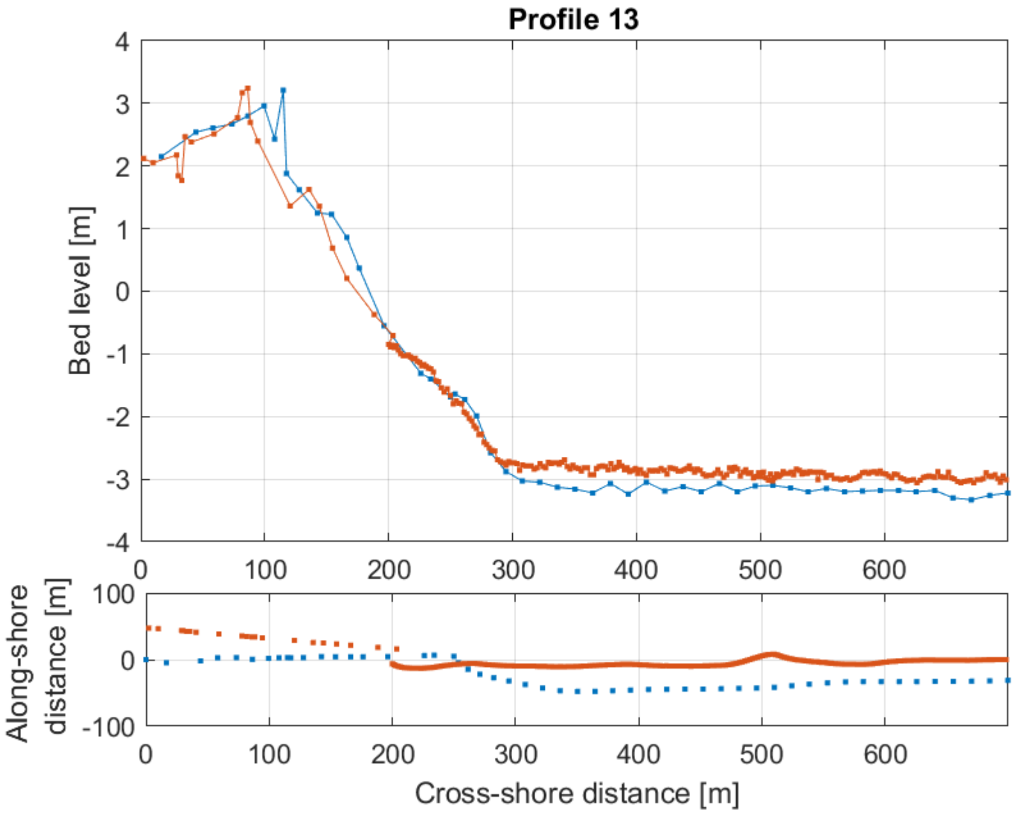
Profile 13
Bed level [m]
Along-shore distance [m]
Cross-shore distance [m]

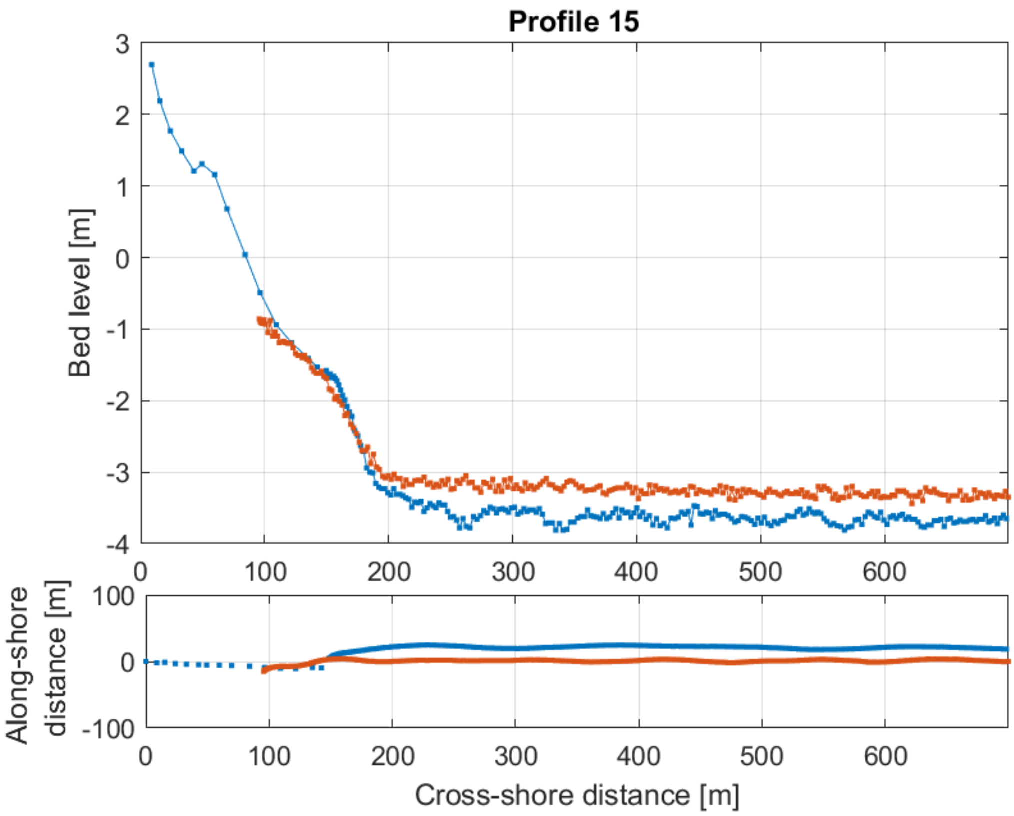
Profile 15
Bed level [m]
Along-shore distance [m]
Cross-shore distance [m]

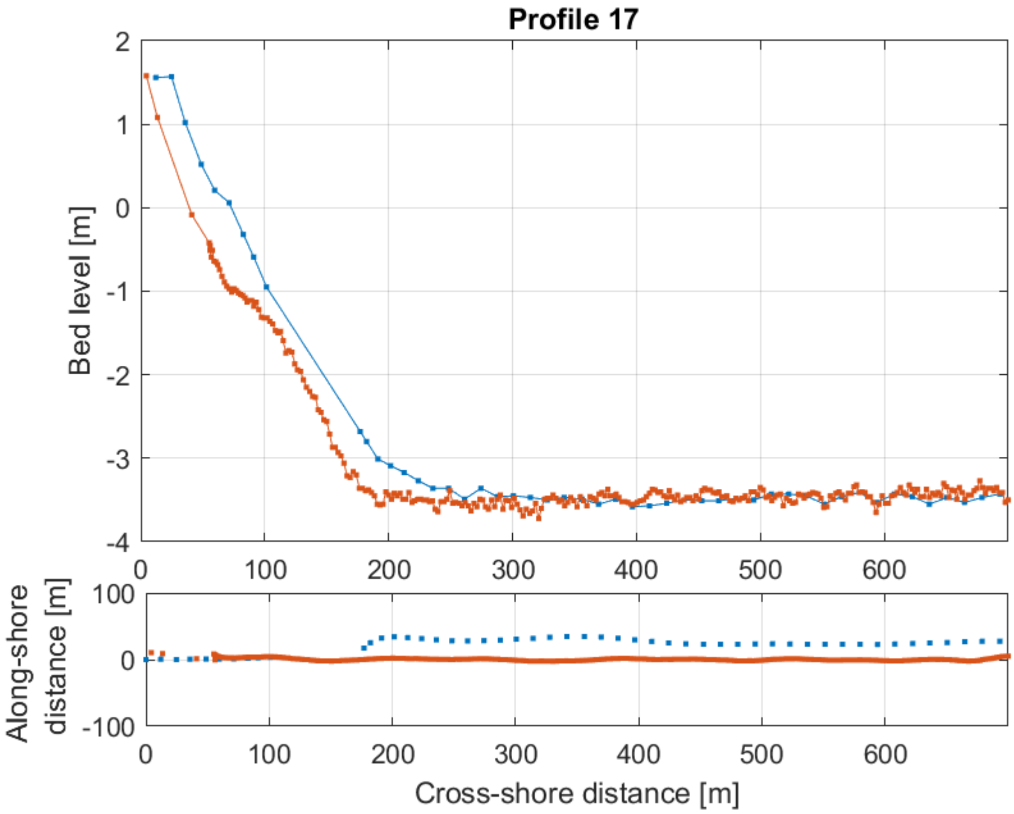

Profile 17
Bed level [m]
2
1
0
-1
-2
-3
-4
0
100
200
300
400
500
600
Along-shore distance [m]
100
0
-100
Cross-shore distance [m]

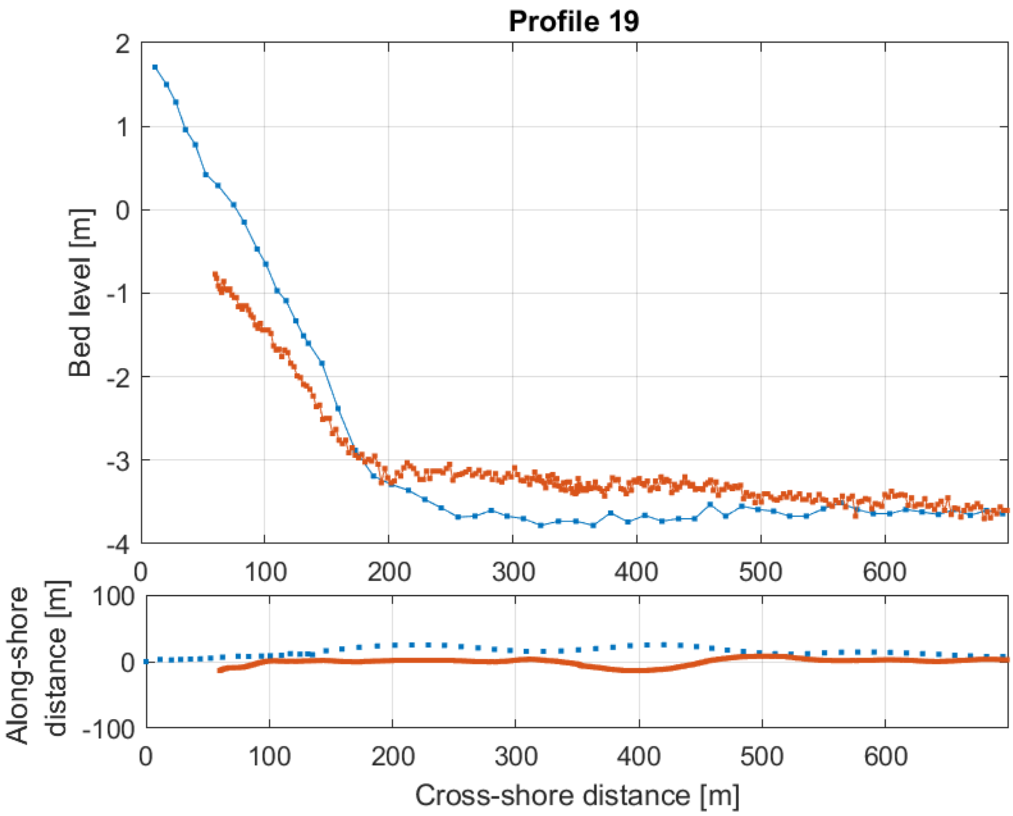

Profile 19
Bed level [m]
2
1
0
-1
-2
-3
-4
0
100
200
300
400
500
600
Along-shore distance [m]
100
0
-100
Cross-shore distance [m]

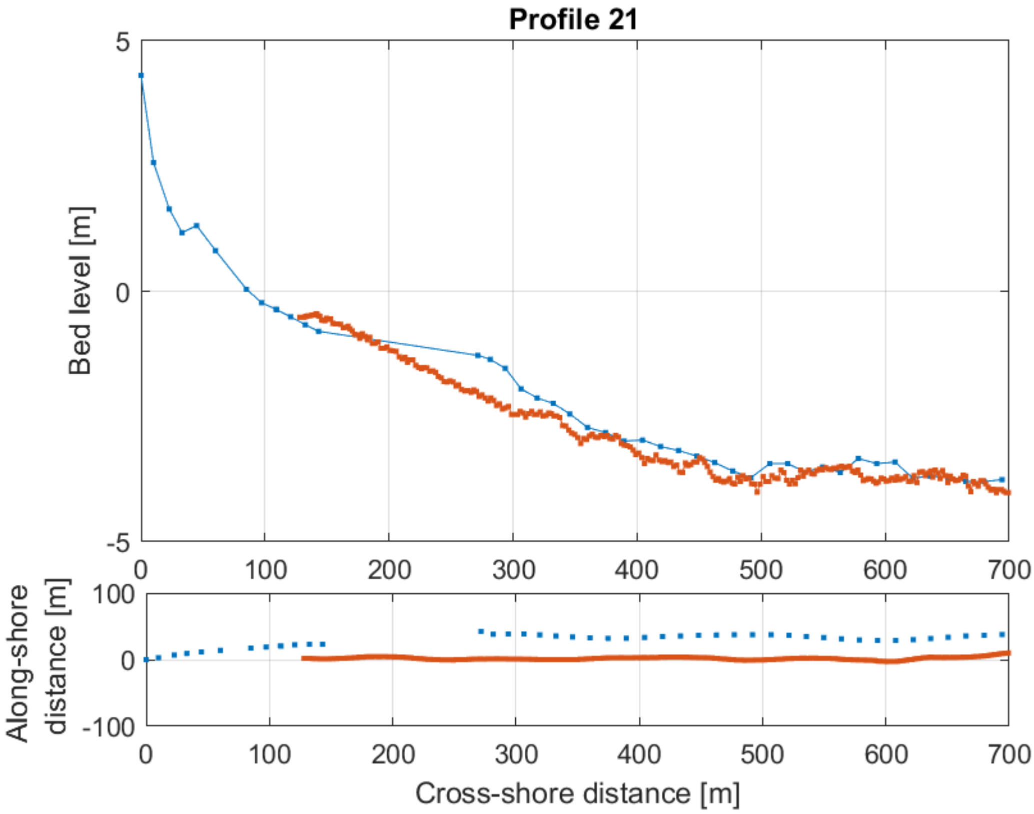

Profile 21
Bed level [m]
5
0
-5
0
100
200
300
400
500
600
700
Along-shore distance [m]
100
0
-100
Cross-shore distance [m]

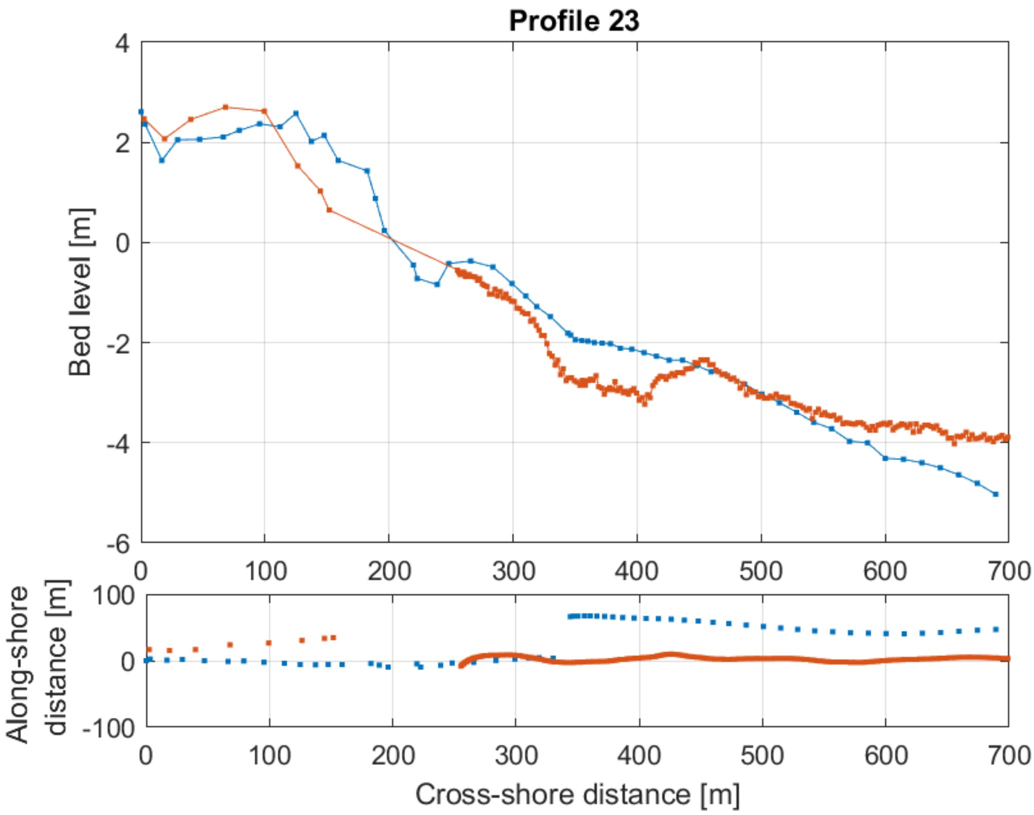

Profile 23
Bed level [m]
4
2
0
-2
-4
-6
0
100
200
300
400
500
600
700
Along-shore distance [m]
100
0
-100
Cross-shore distance [m]

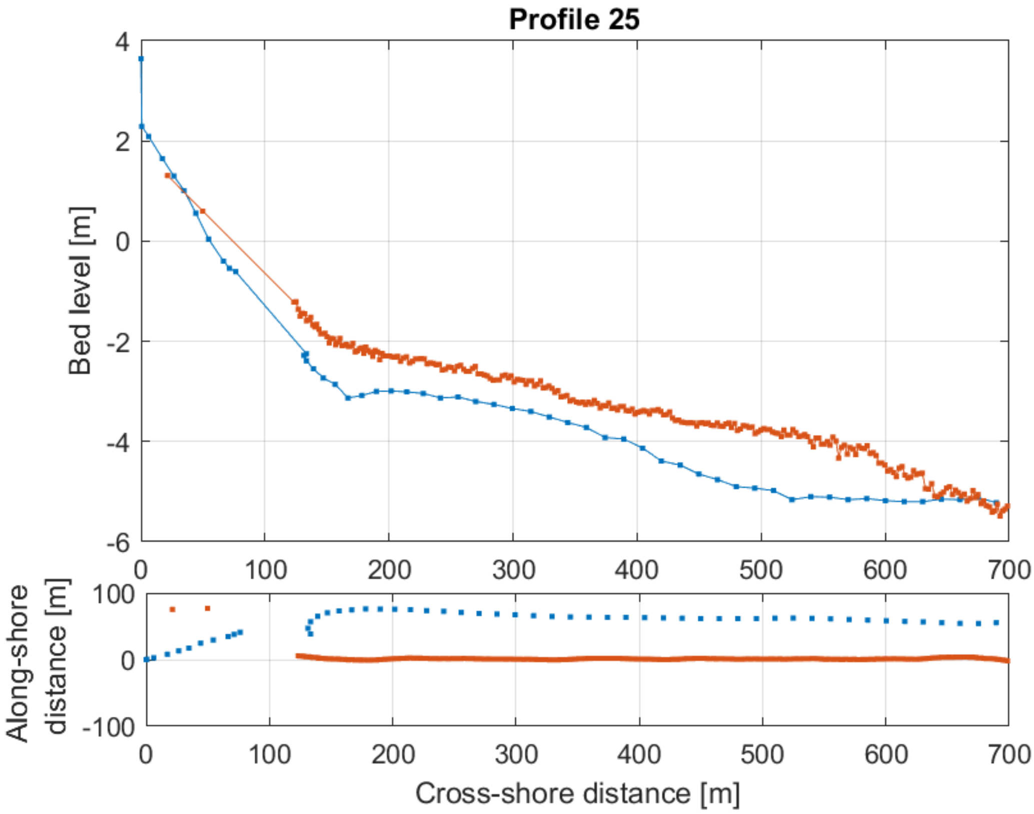

Profile 25
Bed level [m]
4
2
0
-2
-4
-6
0
100
200
300
400
500
600
700
Along-shore distance [m]
100
0
-100
Cross-shore distance [m]